

# **Assessment and Investigation of the Beach and Dune Conditions at South Padre Island**

## **Phase 2 Report: Modeling Future Conditions of the Beach and Dunes**

*Prepared for*  
**City of South Padre Island**  
ATTN: Kristina Boburka, Shoreline Director  
4601 Padre Boulevard  
South Padre Island, TX 78597

*Prepared by*  
The logo for Integral Consulting Inc. features the word "integral" in a bold, lowercase, sans-serif font. A thin, curved line starts from the bottom of the letter "i" and loops around to the right, ending under the letter "l". Below the word "integral" is the text "consulting inc." in a smaller, lowercase, sans-serif font.  
1790 Hughes Landing Blvd.  
Suite 400  
The Woodlands, TX 77380

November 19, 2021

## CONTENTS

<b>LIST OF FIGURES.....</b>	<b>iii</b>
<b>LIST OF TABLES.....</b>	<b>v</b>
<b>ACRONYMS AND ABBREVIATIONS.....</b>	<b>vi</b>
<b>1 INTRODUCTION.....</b>	<b>1-1</b>
<b>2 COASTAL PROCESSES AND HAZARDS.....</b>	<b>2-1</b>
2.1 TIDES AND WATER LEVELS.....	2-1
2.2 WAVES.....	2-2
2.3 SEA LEVEL RISE .....	2-3
<b>3 COASTAL EROSION ASSESSMENT .....</b>	<b>3-1</b>
<b>4 ANALYSIS TRANSECTS .....</b>	<b>4-1</b>
<b>5 XBEACH MODELING .....</b>	<b>5-1</b>
5.1 XBEACH GRID .....	5-1
5.2 XBEACH BOUNDARY CONDITIONS .....	5-1
5.2.1 Extreme Value Analysis.....	5-1
5.3 XBEACH RESULTS .....	5-4
5.3.1 Beach Width.....	5-5
5.3.2 Shoreline and Dune Toe Position Change.....	5-6
5.3.3 Dune Crest Height .....	5-9
5.3.4 Maximum Wave Run-up.....	5-10
5.3.5 Individual Profiles.....	5-11
5.4 MODEL UNCERTAINTY .....	5-32
<b>6 SUMMARY OF FINDINGS.....</b>	<b>6-1</b>
<b>7 RECOMMENDATIONS AND NEXT STEPS.....</b>	<b>7-1</b>
<b>8 REFERENCES .....</b>	<b>8-1</b>

## LIST OF FIGURES

- Figure 1-1. Workflow for Informing a Beach Maintenance Plan that Includes Multiple Phases to Achieve an Actionable Outcome
- Figure 2-1. Conceptual Diagram of the Components of Total Water Level. Image courtesy of Our Coast Our Future Web Platform (Point Blue and USGS 2021).
- Figure 3-1. Relative Sea Level Trend at the South Padre Island, Texas, NOAA Tide Gauge (8779748)
- Figure 4-1. Selected SPI Shoreline Profiles with Mean Sea Level Line
- Figure 5-1. Full Record of Wave Height, Wave Period, and Wave Direction including Average Values from NOAA Buoy 42020
- Figure 5-2. Time Varying Water Level Boundary Condition Applied to XBeach Simulations
- Figure 5-3. Initial Still Water Level and Bed Elevation for Profile CBI-03. MSL Datum Shown for Reference.
- Figure 5-4. Predicted Shoreline Elevation for CBI-03 after 30 Hours of Exposure to a 2-Year Storm Event and 3 SLR Scenarios
- Figure 5-5. Predicted Shoreline Elevation for CBI-03 after 30 Hours of Exposure to a 10-Year Storm Event and 3 SLR Scenarios
- Figure 5-6. Predicted Shoreline Elevation for CBI-03 after 30 Hours of Exposure to a 100-Year Storm Event and 3 SLR Scenarios
- Figure 5-7. Predicted Shoreline Elevation for CBI-06 after 30 Hours of Exposure to a 2-Year Storm Event and 3 SLR Scenarios
- Figure 5-8. Predicted Shoreline Elevation for CBI-06 after 30 Hours of Exposure to a 10-Year Storm Event and 3 SLR Scenarios
- Figure 5-9. Predicted Shoreline Elevation for CBI-06 after 30 Hours of Exposure to a 100-Year Storm Event and 3 SLR Scenarios
- Figure 5-10. Predicted Shoreline Elevation for CBI-13 after 30 Hours of Exposure to a 2-Year Storm Event and 3 SLR Scenarios
- Figure 5-11. Predicted Shoreline Elevation for CBI-13 after 30 Hours of Exposure to a 10-Year Storm Event and 3 SLR Scenarios
- Figure 5-12. Predicted Shoreline Elevation for CBI-13 after 30 Hours of Exposure to a 100-Year Storm Event and 3 SLR Scenarios
- Figure 5-13. Predicted Shoreline Elevation for CBI-17 after 30 Hours of Exposure to a 2-Year Storm Event and 3 SLR Scenarios

- Figure 5-14. Predicted Shoreline Elevation for CBI-17 after 30 Hours of Exposure to a 10-Year Storm Event and 3 SLR Scenarios
- Figure 5-15. Predicted Shoreline Elevation for CBI-17 after 30 Hours of Exposure to a 100-Year Storm Event and 3 SLR Scenarios
- Figure 5-16. Predicted Shoreline Elevation for CBI-22 after 30 Hours of Exposure to a 2-Year Storm Event and 3 SLR Scenarios
- Figure 5-17. Predicted Shoreline Elevation for CBI-22 after 30 Hours of Exposure to a 10-Year Storm Event and 3 SLR Scenarios
- Figure 5-18. Predicted Shoreline Elevation for CBI-22 after 30 Hours of Exposure to a 100-Year Storm Event and 3 SLR Scenarios
- Figure 5-19. Predicted Shoreline Elevation for CBI-24 after 30 Hours of Exposure to a 2-Year Storm Event and 3 SLR Scenarios
- Figure 5-20. Predicted Shoreline Elevation for CBI-24 after 30 Hours of Exposure to a 10-Year Storm Event and 3 SLR Scenarios
- Figure 5-21. Predicted Shoreline Elevation for CBI-24 after 30 Hours of Exposure to a 100-Year Storm Event and 3 SLR Scenarios

## **LIST OF TABLES**

Table 3-1.	Future Sea Level Rise Projections at the South Padre Island, Texas, Coast Guard Station based on NOAA 2017 guidance
Table 5-1.	Wave Height Return Period Values from EVA for the Offshore NOAA Buoy
Table 5-2.	Nearshore Significant Wave Height used for Selected Profiles (feet)
Table 5-3.	Predicted Change in Beach Width, in feet, for the 2-Year Wave Event
Table 5-4.	Predicted Change in Beach Width, in feet, for the 10-Year Wave Event
Table 5-5.	Predicted Change in Beach Width, in feet, for the 100-Year Wave Event
Table 5-6.	Predicted Change in Shoreline Position, in feet, for the 2-Year Wave Event
Table 5-7.	Predicted Change in Shoreline Position, in feet, for the 10-Year Wave Event
Table 5-8.	Predicted Change in Shoreline Position, in feet, for the 100-Year Wave Event
Table 5-9.	Predicted Change in Dune Toe Position, in feet, for the 2-Year Wave Event
Table 5-10.	Predicted Change in Dune Toe Position, in feet, for the 10-Year Wave Event
Table 5-11.	Predicted Change in Dune Toe Position, in feet, for the 100-Year Wave Event
Table 5-12.	Predicted Change in Dune Crest Height, in feet, for the 2-Year Wave Event
Table 5-13.	Predicted Change in Dune Crest Height, in feet, for the 10-Year Wave Event
Table 5-14.	Predicted Change in Dune Crest Height, in feet, for the 100-Year Wave Event
Table 5-15.	Predicted Maximum Wave Run-up, in feet NAVD88, for the 2-Year Wave Event
Table 5-16.	Predicted Maximum Wave Run-up, in feet NAVD88, for the 10-Year Wave Event
Table 5-17.	Predicted Maximum Wave Run-up, in feet NAVD88, for the 100-Year Wave Event

## **ACRONYMS AND ABBREVIATIONS**

1-D	one-dimensional
ADAPT	Adaptation Decision and Planning Tool
EVA	extreme value analysis
GoM	Gulf of Mexico
Integral	Integral Consulting Inc.
MSL	mean sea level
NAVD88	North American Vertical Datum of 1988
NOAA	National Oceanic and Atmospheric Administration
QA/QC	quality assurance and quality control
SLR	sea level rise
SPI	South Padre Island
SWL	still water level
TWL	total water level
USGS	U.S. Geological Survey

# **1 INTRODUCTION**

South Padre Island (SPI) is a narrow, low-relief barrier island along the south Texas coastline that is impacted frequently by erosive winter storm events and infrequent but extremely damaging major hurricanes. Relative rates of sea level rise (SLR) along the Texas coastline are higher than global averages due to subsidence, which exacerbates flooding and increases the inland incursion of storm waves. The dune field that backs the beach along the City of SPI coastline from the Brazos-Santiago Pass to the northern end of the City limits is discontinuous due to numerous beach access points and removal of sand by beachfront property owners. The present dune system is composed of a semi-natural dune field that varies in elevation and width alongshore, and has an extensive vegetation-planting program that helps to provide some resistance to dune erosion.

Scarping of the beach and dune is common in the winter, particularly towards the northern, more erosive part of the beach system. Overall, the beach-dune system provides critical protection to the community of SPI from storm waves and elevated water levels. The beaches and dunes are nourished and planted on a regular basis, thus maintaining a first line of protection for the City and its infrastructure from storm events.

Integral Consulting Inc. (Integral) was awarded a contract with SPI in 2020 to assess and investigate the beach and dune conditions at SPI. The project is being undertaken in four phases (Figure 1-1) following an Integral-developed framework called Coastal ADAPT (Adaptation Decision and Planning Tool) that uses a variety of modeling approaches to examine adaptation options for increasing resiliency to coastal hazards and SLR-related climate change risks. Phase 2, the focus of this report, presents the outcomes of modeling of future possible responses of the beach and dunes at SPI.

Integral offers unique experience, familiarity with relevant data, and decades of modeling experience grounded in locally proven scientific insight into the complex dynamics at play along the southeast coast of Texas. We applied advanced state-of-the-science modeling, incorporating measured data to accurately simulate waves along the SPI coastline. To assess the resiliency of the various dune configurations to an array of storm events, from mild to severe, and identify potential changes to the profiles, XBeach geomorphic modeling was performed (discussed in Section 1). This report provides the results and interpretation of the XBeach modeling, and provides recommendations for maintenance of the beach and dunes based on the historical response reported in Phase 1 of this project and the expected response in the future based on the modeling outcomes.

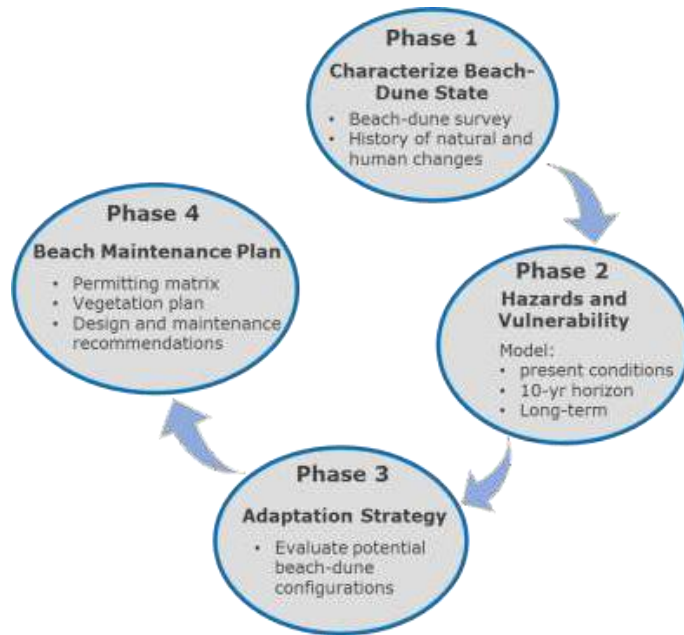


Figure 1-1. Workflow for Informing a Beach Maintenance Plan that Includes Multiple Phases to Achieve an Actionable Outcome

## 2 COASTAL PROCESSES AND HAZARDS

Coastal processes along SPI that create coastal hazards include tides, waves, and related storm conditions. An important measure of coastal hazards is the total water level (TWL; Figure 2-1) elevation—the combined effect of wave run-up height, storm surge, tides, and sea level elevations. River discharge is not a contributing factor to TWL at SPI. A combination of large waves occurring at high tides during storm conditions pose the largest potential to impact coastal erosion. As sea levels rise, both the wave run-up dynamics and the tide elevations will change leading to higher total water levels for longer durations. Each coastal process is summarized briefly below.

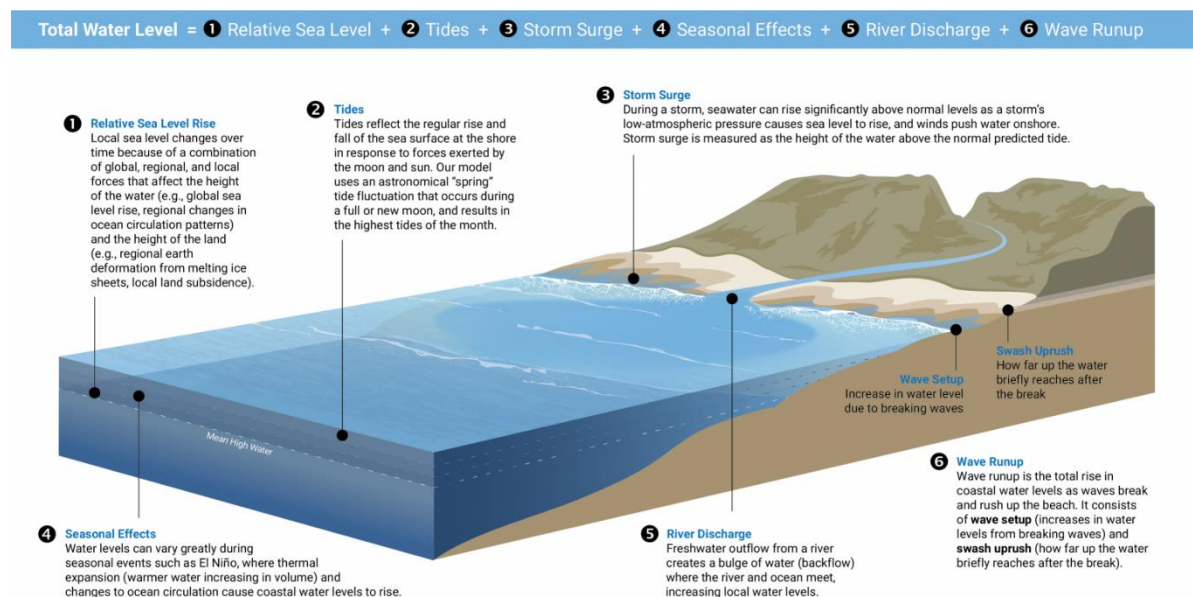


Figure 2-1. Conceptual Diagram of the Components of Total Water Level. Image courtesy of Our Coast Our Future Web Platform (Point Blue and USGS 2021).

### 2.1 TIDES AND WATER LEVELS

The closest National Oceanic and Atmospheric Administration (NOAA) tide gauge station is located at the entrance to the Brazos Santiago ship channel. Tides in the area are a diurnal type, meaning there is one high and one low tide each day. Tides are driven predominantly by the gravitational pull of the sun and the moon with elevations based on a tidal epoch, a 19-year period of which average tidal elevations are statistically analyzed. These tidal elevations are reported in either a tidal datum or a fixed vertical reference datum. Tidal datum elevations are typically relative to mean lower low water—the average of lowest low tides—a useful measurement for navigation purposes. A fixed vertical reference datum is established using

geodetic land-based measurements. For this study, elevations will be reported in fixed land-based vertical reference datum using the North American Vertical Datum of 1988 (NAVD88).

Tide elevations vary monthly and annually based on the lunar orbit and solar positioning. During new and full moon when the gravitational pull of the sun and moon are aligned, spring tides have a higher tide range. During certain atmospheric conditions or wind conditions, tide observations can be much higher than predicted tides due to storm surge components. Still water level (SWL) is the term used to describe the elevation of the tide and the combination of non-wave components. Future SLR rise will raise the SWL elevations, thus affecting the height and extent of the potential for coastal erosion.

## **2.2 WAVES**

Waves, created by distant and local winds, are one of the key drivers of wave run-up and resulting coastal change. Local wind-driven seas typically develop rapidly when low pressure systems track near a locale, especially in the summer and fall months during hurricane season, or when strong sea breezes are generated during the spring and summer. Although the mean wave climate is modulated by winter cold fronts, the most extreme events are related to hurricanes (Appendini et al. 2014).

When distantly generated waves approach the coast as swell, they interact with coastal and bathymetric features. A wave measured at a buoy offshore in deep water is quite different than one that breaks at the coast near SPI. The Yucatan Peninsula, for example, may block swell from the south, while a large northeast or east swell from an offshore storm or hurricane may approach SPI leading to an increased potential for coastal erosion. Modeling of the changing waves based on bathymetry and swell conditions is called wave transformation and was an important modeling component to assessing vulnerabilities for this project.

Waves break offshore in depths that are related to the wave height and the wave period. In general, the bigger the wave and the longer the wave period, the deeper the water in which the wave will break. Smaller waves can travel much closer to shore before breaking and often pose more risk of causing damage than the biggest waves. Once the wave breaks, it runs up the shoreline and the slopes and roughness affect its elevation and inland extent across the surf zone and beach. Depending on the frequency of breaking waves, wave setup can occur when a series of breaking waves can pile up water allowing subsequent waves to travel closer to shore on the piled-up water before breaking with more energy. As sea levels rise, not only will the SWL be affected, but the deeper water close to shore will allow waves to break closer to shore with less potential to dissipate the wave energy.

## 2.3 SEA LEVEL RISE

Increases in greenhouse gas emissions, primarily from the burning of fossil fuels, are contributing to an increase in atmospheric and ocean temperatures, causing ocean waters to warm and expand, and continental glaciers and the ice sheets of Greenland and Antarctica to lose ice mass and melt. As a result, the global rate of SLR has increased to rates of about 0.15 in./year between 1993 and 2018 (Nerem et al. 2018).

However, SLR is not the same everywhere around the world. Because of local differences in tectonic uplift, subsidence caused by oil, gas, and groundwater extraction, as well as sediment deposition and saltwater intrusion, the land itself can move vertically.

Local or relative SLR is more important to this study than global rates of SLR. The tide gauge at the SPI Coast Guard Station (Station ID: 8779748) has recorded a SLR of 0.17 in./yr  $\pm$  0.02 in./yr between 1958 to 2021, equivalent to a change of 1.4 ft in 100 years (Figure 3-1 ). This is equivalent to the average global rate of SLR  $\sim$ 0.15 in./yr; however, this trend, relative to global SLR, will change in the future (IPCC 2021).

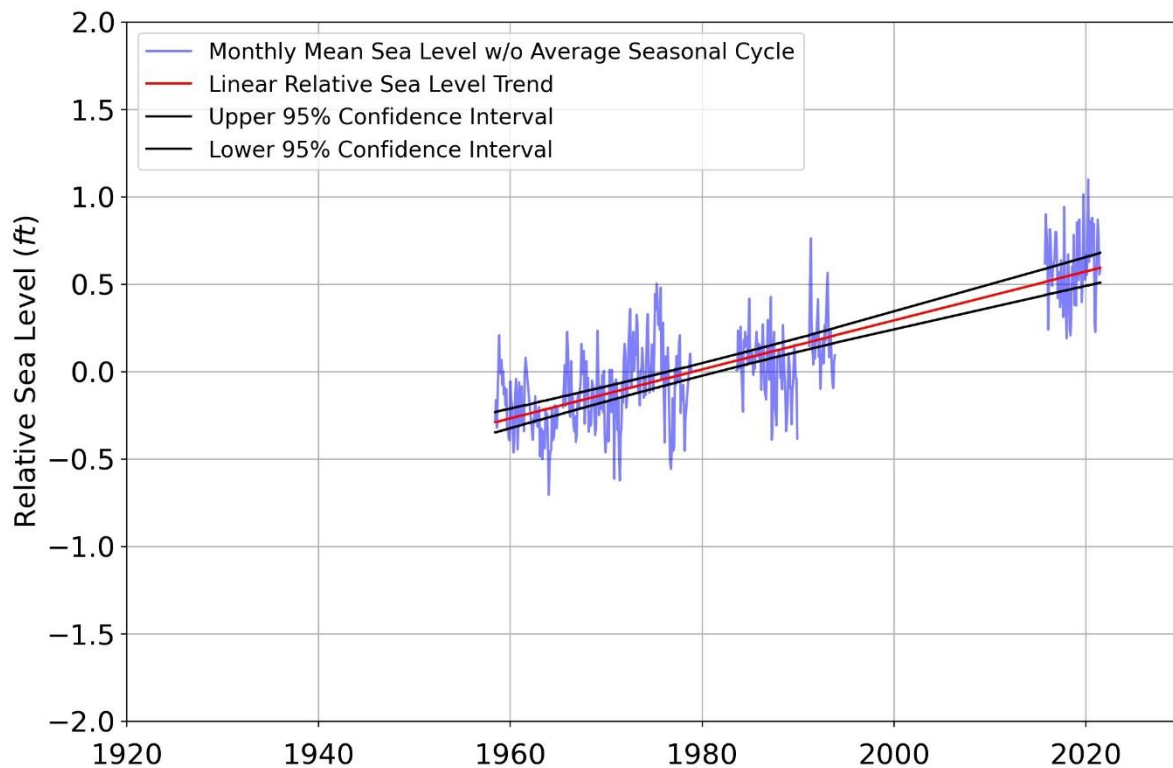


Figure 3-1. Relative Sea Level Trend at the South Padre Island, Texas, NOAA Tide Gauge 8779748. Source: <https://tidesandcurrents.noaa.gov/waterlevels.html?id=8779748>.

### 3 COASTAL EROSION ASSESSMENT

The major technical task of this study was to evaluate the potential for coastal erosion of SPI beaches and dunes for a range of projected storm events in addition to future SLR scenarios. Overall, the methods to conduct this coastal change analysis included assessment of site topographic and nearby bathymetric conditions, the regional wave climate and wave refraction to the shoreline adjacent to the site, and XBeach modeling to predict coastal erosion potential. This section summarizes the methods and focuses on the modeling and the results of the analyses. This study considered the following coastal hazards:

- **Coastal Erosion and Accretion:** Erosion and accretion along the SPI beaches and dunes from projected storm conditions associated with various recurrence frequencies. The different recurrence intervals help better understand the storm frequency over time that the beaches and dunes may be exposed to, and are listed below:
  - 2-year, also referred to as a 50% annual chance storm event
  - 10-year, also referred to as a 10% annual chance storm event
  - 100-year, also referred to as a 1% annual chance storm event.
- **Rising Sea Level:** Rise in the predicted tide levels due to SLR and its influence on coastal change.

NOAA and other government agencies and universities have substantially invested in SLR science that assigns probabilities to various SLR elevations occurring by a certain time in the future (Sweet et al. 2017). For this study, the intermediate-high risk scenario was applied, consistent with existing policy guidance (Table 3-1; Sweet et al. 2017).

Table 3-1. Future Sea Level Rise Projections at the South Padre Island, Texas, Coast Guard Station based on NOAA 2017 guidance

Sea Level Rise Scenario (ft)	Projected Years
0.0	2020 (Baseline Year)
1.54	2040 (Intermediate High)
3.54	2070 (Intermediate High)

## 4 ANALYSIS TRANSECTS

Six shoreline profiles were selected from the 25 profiles analyzed in the historical morphodynamic analysis (see Phase 1 Report “Characterization of the Beach and Dune State”) to perform XBeach simulations and evaluate the coastal change potential. The selected profiles were CBI-03, CBI-06, CBI-13, CBI-17, CBI-22, and CBI-24 (Figure 4-1). These profiles were selected using the June 2021 survey data, carried out as part of the present project. Since CBI-22 was undergoing nourishment during the June 2021 survey, the elevation data for this profile were from the May 2020 survey. The profiles were selected based on unique morphologies and historical behavior to be a subset that is representative of the different distinct morphologies and geography in the area of interest. These include representing the three portions of the island that have been identified in long-term analyses as having variable evolution (south, central, and north). The following describe the specific characteristics of the chosen profiles:

- CBI-03: southern portion of SPI; development set far back (more representative of natural location)
- CBI-06: southern portion of SPI without potential jetty impacts; has experienced consistent vegetation progradation
- CBI-13: central portion of SPI; stable profile morphology
- CBI-17: central portion of SPI; stable profile morphology
- CBI-22: northern portion of SPI; lack of vegetation and dune historically; low dune maintained in more recent times, since ~2008
- CBI-24: northern portion of study area; undeveloped region (no building line); dune field widened and has maintained stable configuration in recent years (2018–2021).

The range of wave conditions within the Gulf of Mexico (GoM) responds to the topography and bathymetry in and along the coastline of SPI. Of primary importance is the site-specific nearshore bathymetric and topographic data along selected beach profiles.

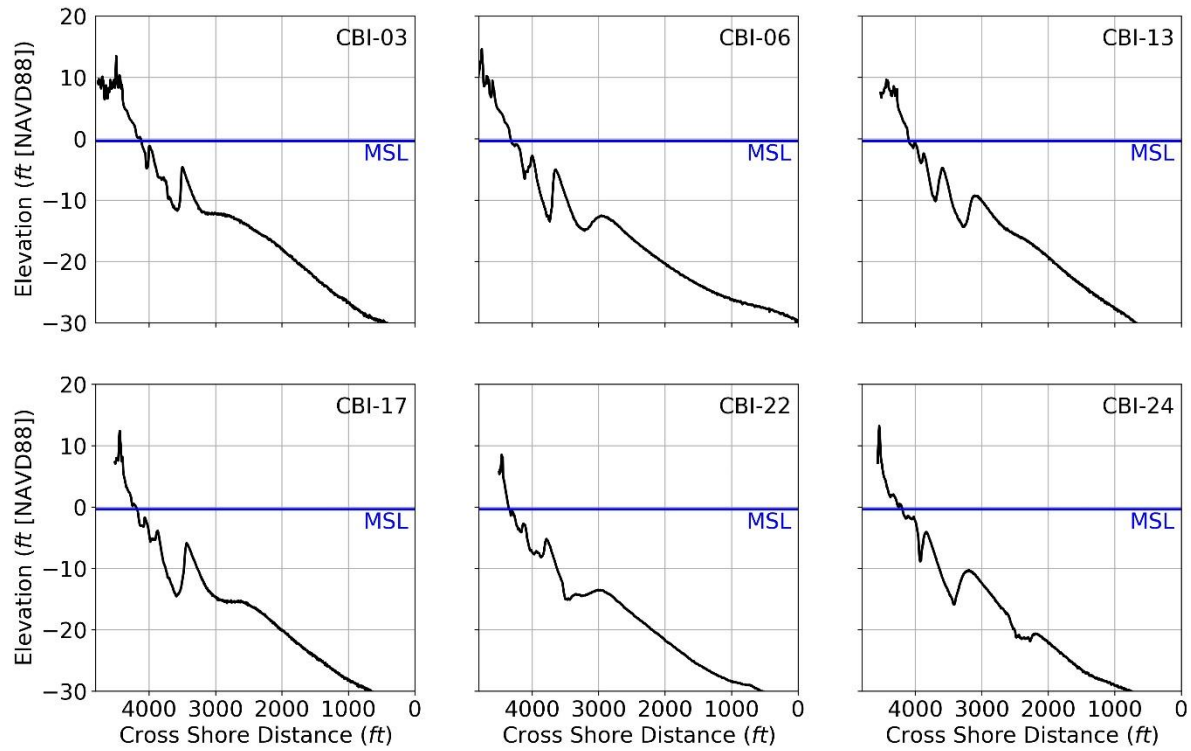


Figure 4-1. Selected SPI Shoreline Profiles with Mean Sea Level Line (June 2021, except CBI-22 in May 2020)

## 5 XBEACH MODELING

XBeach is a numerical model used to predict coastal erosion and accretion, and was used to model coastal change potential along the selected set of shoreline profiles under a range of storm wave and future SLR conditions (Rovelvink et al. 2009). The model assesses the interaction of waves with bathymetry and topography. XBeach is particularly suited for modeling coastal change (e.g., volume, width, elevation) processes on timescales of single storm and wave events; it simulates tidal and wave-driven sediment transport and resulting coastal change, and is a readily available, free, open-source model.

### 5.1 XBEACH GRID

Each of the six selected profiles were discretized into a number of grid cells representing a discrete distance in the cross-shore direction, and each grid cell was assigned an average water depth. There is only a single grid cell in the alongshore direction. The resolution of the grid cells in the cross-shore direction varied from 40 ft at the farthest offshore cells where erosion and accretion are expected to be limited, to 1.6 ft along the beach and dune profile where a majority of the erosion and accretion is expected. The grid configuration is only in the cross-shore direction, and is called the XBeach 1-D, or one-dimensional mode. In the 1-D mode, the model domain represents a single shoreline profile, and longshore transport gradients are ignored. The varying grid spacing and use of XBeach 1-D were used to provide high-resolution predictions along the beach and dune while minimizing the number of offshore grid cells to maintain computational efficiency.

### 5.2 XBEACH BOUNDARY CONDITIONS

At the offshore boundary at each of the XBeach grids, the application of wave conditions can take multiple forms. For this study, at each of the six selected profiles, bulk wave parameters—significant wave height, peak period, wave direction, and a directional spreading factor—accessed from the closest NOAA wave buoy, were applied at the offshore end. The bulk wave parameters were held constant over a 30-hour simulation period to represent the worst case scenario during a selected storm event.

#### 5.2.1 Extreme Value Analysis

The range of wave processes in response to the wide sloping continental shelf along the coast of the GoM necessitates a qualitative and quantitative understanding of existing wave conditions. In an effort to summarize the existing wave conditions along SPI, the full data record from the closest NOAA wave buoy was downloaded and analyzed. This NOAA buoy, station 42020, is located ~68 miles northeast of the Brazos Santiago Channel and the south end of SPI, and has a

data record from 1990–present (Figure 5-1). The NOAA buoy is in 280 ft of water near the edge of the continental shelf and is equipped with sensors to collect meteorological data, water temperature, and directional wave data. Over the full data record at this NOAA buoy, the mean wave height is 4.3 ft, the mean wave period is 6.3 seconds, and the median wave direction is 120°. The median is defined as the middle wave direction of the entire record. To evaluate the impact of extreme storm events on the coastal resiliency of SPI beaches and dunes, extreme values of wave height, representative of an array of storm events, were computed for use in the XBeach model. The extreme value analysis (EVA) provided the highest wave heights for various return periods (e.g., 2, 10, and 100 years) from a 30-year measured data record (Table 5-1).

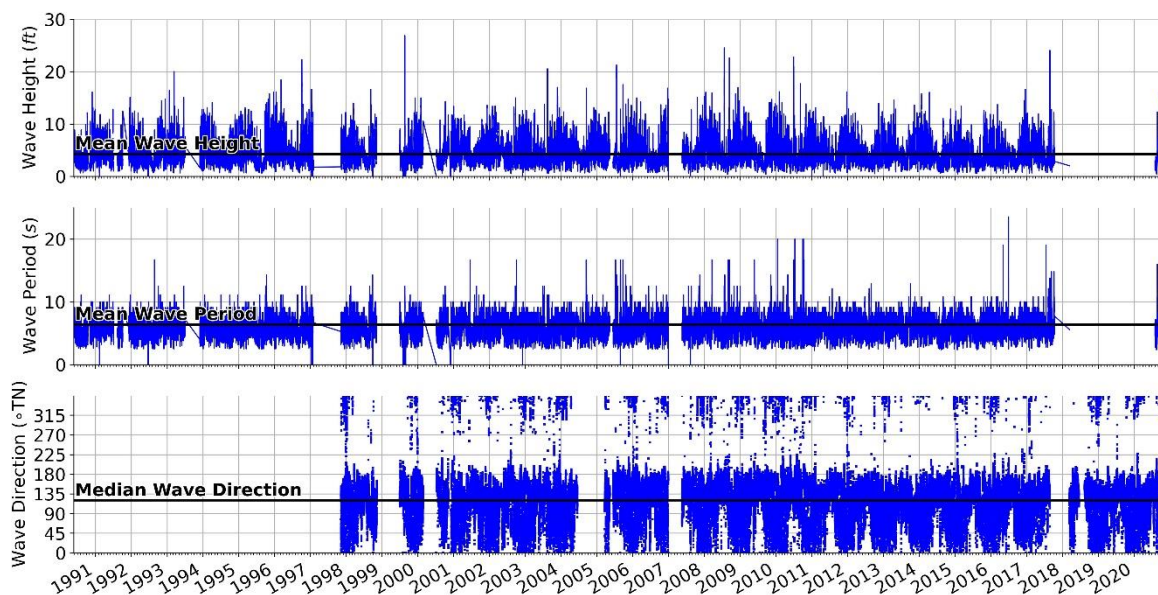


Figure 5-1. Full Record of Wave Height, Wave Period, and Wave Direction including Average Values from NOAA Buoy 42020

Table 5-1. Wave Height Return Period Values from EVA for the Offshore NOAA Buoy

Return Period	Offshore Significant Wave Height (ft)
1-year	16.2
10-year	22.9
100-year	41.7

The NOAA buoy measurements used in the EVA are typically in deep water where the influence of the bathymetry and local nearshore bathymetric features do not affect the waves. Thus, it is critically important to transform the waves from the deep water to the nearshore zone

to evaluate site specific wave exposure. Linear Airy wave theory was used to transform the deep water waves into the nearshore region as shallow water waves, taking into account the effects of the shallower nearshore water depths and profile slope, and how the waves will be influenced. These transformed wave heights were used as the XBeach boundary conditions for the six selected profiles (Table 5-2). The nearshore wave heights, along with the offshore wave heights derived from the EVA, sequentially increase for the 2-, 10-, and 100-year return periods and contribute to increased wave run-up and the potential for beach and dune erosion and accretion. The return period storm events, combined with the three SLR scenarios discussed above, resulted in 54 individual XBeach model simulations representing three different significant storm events and three SLR scenarios along the six selected profiles. The wave period was held constant across the 54 XBeach simulations, set as 16 seconds, a typical wave period generated from an offshore storm event in the Gulf of Mexico. XBeach was set to run for 30 hours, representative of a typical storm event duration, and to capture a full tidal cycle. During the 30-hour period, constant wave and time varying water level boundary conditions were applied.

Table 5-2. Nearshore Significant Wave Height used for Selected Profiles

Return Period	Offshore Significant Wave Height (feet)	Nearshore Significant Wave Height (feet)
2-year	16.2	13.2
10-year	22.9	17.8
100-year	41.7	22.9

In addition to the wave conditions at the offshore boundary, a time-varying water level was applied. A time-varying water level provided a more realistic storm impact, as it would occur over a tidal cycle, and the higher tides would increase the probability of erosion and accretion along the shoreface. These data were selected from the measured data record at NOAA station # 8779749, SPI Brazos Santiago, Texas (Figure 5-2) and subset to a transition from a neap to spring tide. This simulates an increasing water level resulting from storm surge, along with the constant wave conditions.

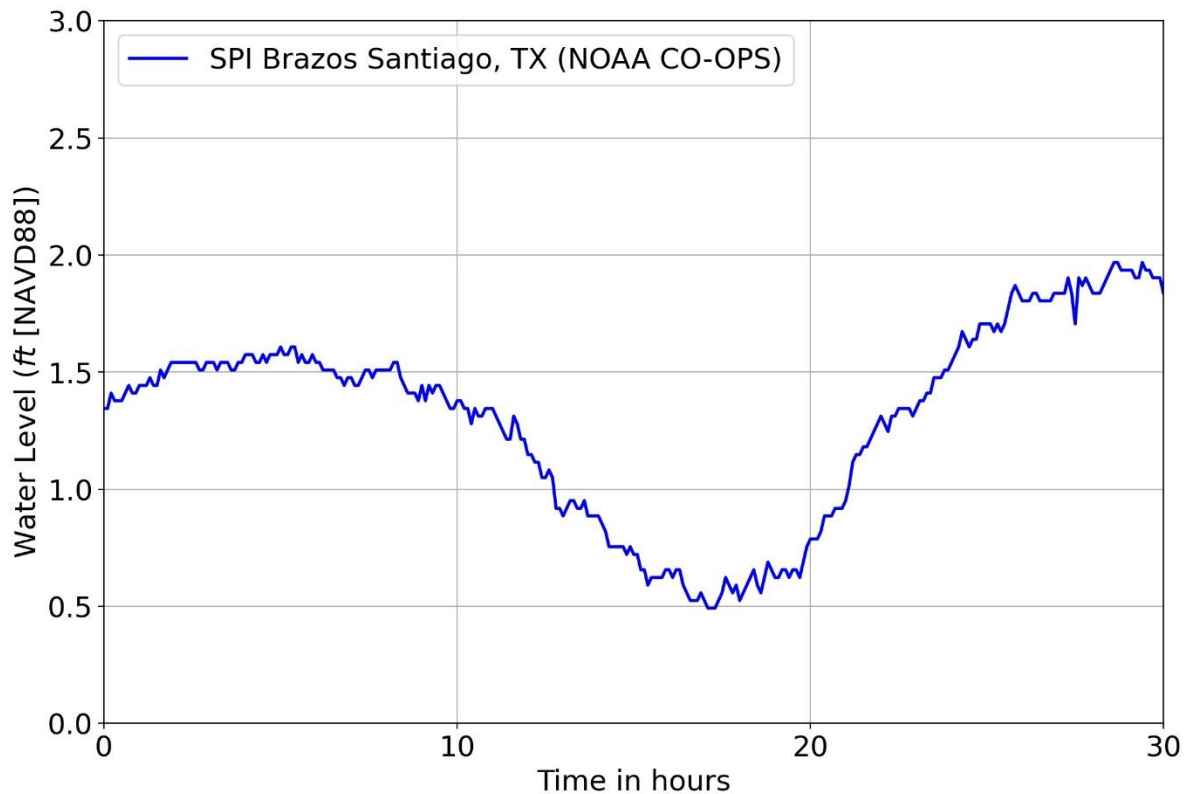


Figure 5-2. Time Varying Water Level Boundary Condition Applied to XBeach Simulations

In addition to the wave and water level boundary conditions, vegetation and sediment physical characteristics were defined along each of the selected profiles. The location of the vegetation line was identified in the beach profile survey data. The vegetation feature in XBeach provides additional roughness for predicting the wave run-up and erosion of the dunes. The sediment physical characteristics (i.e., D50, D90, porosity, and bulk density) were defined based on typical sandy beaches along the Gulf Coast region. These model parameters provide a more realistic sediment bed when simulating erosion and accretion.

### 5.3 XBEACH RESULTS

The model predictions provide an evaluation of coastal erosion and accretion potential along each of the selected profiles due to defined storm events. Each of the 54 simulations were evaluated and quantitative metrics were computed to assess the predicted changes to each profile under various storm conditions and SLR scenarios. The metrics include changes to the beach width, the shoreline position, and the dune toe position. The results of the analyses are presented below.

### 5.3.1 Beach Width

As an initial metric to evaluate the change in each profile over the range of storm events and SLR scenarios, beach width change was computed for the 54 simulations (Tables 5-3 to 5-5). The positive values in the three tables, light to dark blue, represent an increase in beach width, while the negative values, light to dark red, represent a decrease in beach width.

To compute the beach widths, the results from the 54 simulations were run through the Python dune analysis package Pybeach (<https://pybeach.readthedocs.io/en/latest/>). The maximum curvature method (maximum slope change) was chosen to calculate the dune toe and shoreline for each simulation, including the starting profiles. Beach width was then calculated as the distance from the Pybeach-derived dune toe and shoreline. The pre-storm beach width was then subtracted from the post-storm simulated beach width.

Overall, the changes in beach widths are highly variable across profiles, storm events, and SLR scenarios. As reported in the Phase 1 Report “Assessment and Investigation of the Beach and Dune Conditions at South Padre Island” and based on historical analysis, the magnitude of beach width change increases when moving north along SPI, a result consistent with the rates of change derived from beach nourishment and offshore sand placement. The pattern is variable along the coast, with erosion hotspots in the very northern portion of the study area (beyond the extent of the CBI profiles), accretion or low erosion rates (< 0.9 ft/yr) along much of the central portion of the island (CBI-09 to CBI-25), and an area of moderate erosion (-0.4 to -1.4 ft/yr) along the coast from CBI-05 to CBI-09. South of this erosional zone, the shoreline becomes accretional to the inlet jetty.

As shown in Tables 5-3 to 5-5, the beaches were predicted to increase in width in 29 of the 54 profile simulations. Twenty-four profiles showed a decrease in beach width across the simulations and one of the simulations, profile CBI-17 for the 2-year wave event and 2070 SLR scenario, was predicted to have no change (Table 5-3).

Profile CBI-06, near the south end of SPI, was predicted to have the largest increase in beach width, while CBI-24, one of the most northerly profiles, was predicted to have the largest decrease in beach width. An interesting trend shows that the largest changes in beach width are not necessarily during the largest wave events or highest SLR scenarios. This is a result of the influence of bathymetry and topography on the wave run-up and wave forces responsible for coastal erosion and accretion. During the 0.0-ft SLR scenario, smaller waves (e.g., the 10-year wave event) can travel closer to shore before breaking, thus potentially causing more erosion of the beach. During the 2040 and 2070 SLR scenarios, the breaking depths of the profiles change, impacting where the wave breaks, and if it breaks at all. The importance of this finding is that more frequent smaller wave events could increase the potential for coastal erosion. Explanations for increasing beach widths under storm and SLR conditions, when intuitively one might expect to see decreases in the beach width, are two-fold. Sediment can be transported

onshore during storm events and material eroded from the dunes can be deposited on the beach. In the latter case, one would expect there to be measurable erosion of the dune. In this analysis, it appears that where there are large increases in beach width, material is moved from the very shallow submerged portions of the profiles onto the beach.

Table 5-3. Predicted Change in Beach Width, in feet, for the 2-Year Wave Event

Sea Level Rise (ft)	CBI-03	CBI-06	CBI-13	CBI-17	CBI-22	CBI-24
0.00	-31.2	16.4	11.5	-42.7	14.8	13.1
1.54 (2040)	-8.2	52.2	37.3	1.6	14.8	-31.2
3.54 (2070)	-3.3	33.3	66.4	0.0	32.0	4.9

Table 5-4. Predicted Change in Beach Width, in feet, for the 10-Year Wave Event

Sea Level Rise (ft)	CBI-03	CBI-06	CBI-13	CBI-17	CBI-22	CBI-24
0.00	-8.2	21.3	39.4	-36.1	39.4	-42.7
1.54 (2040)	-4.9	18.1	68.0	-18.0	-1.6	-4.9
3.54 (2070)	-3.3	125.1	68.0	-4.9	21.3	-23.0

Table 5-5. Predicted Change in Beach Width, in feet, for the 100-Year Wave Event

Sea Level Rise (ft)	CBI-03	CBI-06	CBI-13	CBI-17	CBI-22	CBI-24
0.00	-45.9	14.8	32.8	-45.9	34.5	-62.3
1.54 (2040)	-36.1	11.5	1.6	-67.3	9.8	-95.1
3.54 (2070)	-13.1	113.2	98.4	6.6	14.8	-70.5

### 5.3.2 Shoreline and Dune Toe Position Change

The computation of the beach width change requires the identification of the shoreline and dune toe position along each profile. In addition to examining the beach width change, we also examined changes in the positions of the shoreline and dune toe, which are presented below. This was conducted for each of the 54 simulations using Pybeach (Tables 5-6 to 5-11). The positive values in the tables, light to dark blue, represent a predicted shoreline advance, or seaward movement, while the negative values, light to dark red, represent a shoreline retreat, or landward movement.

For shoreline position changes (Tables 5-6 to 5-8), 23 of the 54 simulations predicted an advance of the shoreline. On 28 profiles shoreline retreat was predicted, and three simulations predicted no change in the shoreline position. Profile CBI-17 for the 100-year wave event and 2070 SLR scenario, and CBI-13 for the 100-year wave event for the current and 2040 SLR scenarios, had no predicted shoreline position change but did have predicted beach width change (Table 5-8).

Similar to the changes in beach width, profile CBI-06 was predicted to have the largest shoreline advance, during the 2-year wave event and the 2040 SLR scenario (Table 5-6). Across each of the storm wave events and SLR scenarios, profile CBI-06 was predicted to have an advance in its shoreline position. Profile CBI-24 was predicted to have the largest shoreline retreat, which occurs during the 100-year wave event, 2040 SLR scenario (Table 5-8). Most of the remaining simulations were shown to have predicted shoreline retreat.

Table 5-6. Predicted Change in Shoreline Position, in feet, for the 2-Year Wave Event

Sea Level Rise (ft)	CBI-03	CBI-06	CBI-13	CBI-17	CBI-22	CBI-24
0.00	-31.2	16.4	11.5	-42.7	14.8	13.1
1.54 (2040)	-8.2	52.2	37.3	1.6	13.1	-31.2
3.54 (2070)	-3.3	33.3	35.2	-3.3	30.4	1.6

Table 5-7. Predicted Change in Shoreline Position, in feet, for the 10-Year Wave Event

Sea Level Rise (ft)	CBI-03	CBI-06	CBI-13	CBI-17	CBI-22	CBI-24
0.00	-8.2	21.3	6.6	-36.1	18.0	-42.7
1.54 (2040)	-4.9	18.1	35.2	-18.0	23.0	-4.9
3.54 (2070)	-3.3	31.6	35.2	-13.1	19.7	-29.5

Table 5-8. Predicted Change in Shoreline Position, in feet, for the 100-Year Wave Event

Sea Level Rise (ft)	CBI-03	CBI-06	CBI-13	CBI-17	CBI-22	CBI-24
0.00	-45.9	14.8	0.0	-45.9	18.0	-62.3
1.54 (2040)	-36.1	11.5	0.0	-41.0	1.6	-100.1
3.54 (2070)	-14.8	19.7	16.4	0.0	13.1	-80.4

The change in position of the dune toe was also computed for each of the 54 simulations. The positive values in the three tables, light to dark blue, represent a predicted dune toe advance, or seaward movement, while the negative values, light to dark red, represent a landward dune toe retreat.

As shown in Tables 5-9 to 5-11, 29 of the 54 simulations predicted no change in dune toe position. An additional 13 simulations predicted less than 10 ft of dune toe retreat. The dune at the southernmost profile, CBI-03, was not predicted to be impacted during the 2- or 10-year wave events under the three SLR scenarios. Moving northwards along the SPI coastline, the dune generally was predicted to be impacted during the 2-year wave event and the 2070 SLR scenario. During the 10-year and 100-year wave events, as would be expected, the dunes were impacted during the three SLR scenarios for profiles CBI-06, -13, -17, -22, and -24 (Tables 5-10 and 5-11).

As a note, the -32.8-ft change for the four simulations at profile CBI-13 are a result of the Pybeach analysis selecting the dune toe location landward of where the starting profile dune toe was located. After a post-processing analysis, it was found that the dune toe was minimally impacted during these four simulations. In addition, the 24.6-ft advance of the dune toe predicted for profile CBI-22 (Table 5-10) was a result of Pybeach selecting a dune toe location shoreward of the actual dune toe. After a post-processing analysis, it was found that the dune toe position did retreat similar to the 10-year wave event and present SLR scenario (Table 5-10). This update would result in the predicted beach width change for profile CBI-22, during the 10-year wave event and 2040 SLR scenario, to increase.

Table 5-9. Predicted Change in the Dune Toe Position, in feet, for the 2-Year Wave Event

Sea Level Rise (ft)	CBI-03	CBI-06	CBI-13	CBI-17	CBI-22	CBI-24
0.00	0.0	0.0	0.0	0.0	0.0	0.0
1.54 (2040)	0.0	0.0	0.0	0.0	-1.6	0.0
3.54 (2070)	0.0	0.0	-31.2	-3.3	-1.6	-3.3

Table 5-10. Predicted Change in the Dune Toe Position, in feet, for the 10-Year Wave Event

Sea Level Rise (ft)	CBI-03	CBI-06	CBI-13	CBI-17	CBI-22	CBI-24
0.00	0.0	0.0	-32.8	0.0	-21.3	0.0
1.54 (2040)	0.0	0.0	-32.8	0.0	24.6	0.0
3.54 (2070)	0.0	-93.5	-32.8	-8.2	-1.6	-6.6

Table 5-11. Predicted Change in the Dune Toe Position, in feet, for the 100-Year Wave Event

Sea Level Rise (ft)	CBI-03	CBI-06	CBI-13	CBI-17	CBI-22	CBI-24
0.00	0.0	0.0	-32.8	0.0	-16.4	0.0
1.54 (2040)	0.0	0.0	-1.6	26.2	-8.2	-4.9
3.54 (2070)	-1.64	-93.5	-82.0	-6.6	-1.6	-9.8

Profile CBI-13 showed substantial erosion of the dune toe during the 10- and 100-year wave events and for the three SLR scenarios (Tables 5-10 and 5-11). The large increase in beach width for CBI-13 was a result of an advance of the shoreline position, but the sediment for that accretion likely eroded from the dune toe.

The largest predicted advance in the position of the dune toe was along profile CBI-22 for the 10-year wave event and 2040 SLR scenario (Table 5-10). The same profile was predicted to have

a similar advance in its shoreline position, which resulted in a minimal change in the beach width.

### 5.3.3 Dune Crest Height

The final quantitative metric evaluated for this study, change in dune crest height, was computed independent of beach width. The dune crest height represents the highest elevation along the dune of each of the selected profiles. The dune crest height change was computed for each of the 54 simulations by using Pybeach to extract the pre-storm and post-storm dune crest elevations, and then the pre-storm dune crest elevation was subtracted from the post-storm dune crest elevation (Tables 5-12 to 5-14). The negative values in the three tables below, highlighted in light to dark red, represent a decrease in dune crest height. There were no predicted increases in dune crest height.

Table 5-12. Predicted Change in the Dune Crest Height, in feet, for the 2-Year Wave Event

Sea Level Rise (ft)	CBI-03	CBI-06	CBI-13	CBI-17	CBI-22	CBI-24
0.00	0.0	0.0	0.0	0.0	0.0	0.0
1.54 (2040)	0.0	0.0	0.0	0.0	0.0	0.0
3.54 (2070)	0.0	0.0	0.0	0.0	-3.3	0.0

Table 5-13. Predicted Change in the Dune Crest Height, in feet, for the 10-Year Wave Event

Sea Level Rise (ft)	CBI-03	CBI-06	CBI-13	CBI-17	CBI-22	CBI-24
0.00	0.0	0.0	0.0	0.0	-0.2	0.0
1.54 (2040)	0.0	0.0	0.0	0.0	-0.1	0.0
3.54 (2070)	0.0	0.0	0.0	0.0	-3.3	0.0

Table 5-14. Predicted Change in the Dune Crest Height, in feet, for the 100-Year Wave Event

Sea Level Rise (ft)	CBI-03	CBI-06	CBI-13	CBI-17	CBI-22	CBI-24
0.00	0.0	0.0	0.0	0.0	0.0	0.0
1.54 (2040)	0.0	0.0	0.0	0.0	-3.2	0.0
3.54 (2070)	0.0	0.0	0.0	0.0	-3.3	0.0

As shown in Tables 5-12 to 5-14, 48 of the 54 simulations had no predicted change in dune crest height. Two of the simulations predicted decreases in dune crest elevation of 0.2 ft or less. CBI-22 was the only profile where the dune crest height was predicted to erode. CBI-22 had the lowest starting dune crest height of the six selected profiles. The changes in dune crest height at

CBI-22 signify that some overtopping of the dune was predicted, though mostly during the 2070 SLR scenario for the three wave events, and during the 2040 SLR scenario only during the 100-year wave event. Overtopping can lead to flooding in the dune swales, potentially impacting dune fauna and flora. Dune crest elevation changes were predicted for profile CBI-22 with the largest changes predicted for the three wave events during the 2070 SLR scenario, when the dune crest elevation decreases by 3.3 ft.

### 5.3.4 Maximum Wave Run-up

For the maximum wave run-up analysis, wave run-up elevation along each profile is based on the TWL, a combination of tides, surge, and wave conditions (Figure 2-1). The TWL analysis considers multiple worst case scenarios, which include a range of SLR scenarios and storm wave events at differing recurrence intervals (2-year, 10-year, and 100-year). The combination of SLR and wave heights along each profile were evaluated using XBeach to predict potential wave run-up elevation and inland flood exposure to SPI in the future.

The predicted maximum wave run-up along each of the profiles, for each of the storm scenarios, and each of SLR scenarios are presented in Tables 5-15 to 5-17. Overall, the XBeach results illustrate that, in general and as expected, as the offshore wave heights increase and as the SWL elevation increases with SLR, the potential wave run-up height increases.

Wave run-up elevation values during the 100-year storm events with moderate (2040) and high (2070) SLR are approaching elevations in which dune overtopping may occur. As a note, the predicted maximum run-up along profile CBI-03 during the 10-year wave event was higher for the 2040 SLR scenario as compared to the 2070 SLR scenario (Table 5-16). The reason is a result of the influence of bathymetry and topography on the breaking waves. With the deeper water depths during the 2070 SLR scenario, the influence of the seafloor on the wave is reduced; as a result, the wave may not break along the shoreface and not create as high of run-up compared to the shallower water depths.

Table 5-15. Predicted Maximum Wave Run-up, in feet NAVD88, for the 2-Year Wave Event

Sea Level Rise (ft)	CBI-03	CBI-06	CBI-13	CBI-17	CBI-22	CBI-24
Pre-Storm Dune Crest Elevation (ft)	13.35	14.57	9.58	12.37	8.5	13.12
0.00	5.4	6.0	4.4	5.3	5.3	3.9
1.54 (2040)	5.3	5.6	7.3	6.4	8.6	5.9
3.54 (2070)	7.2	6.2	8.1	8.3	8.6	6.5

Table 5-16. Predicted Maximum Wave Run-up, in feet NAVD88, for the 10-Year Wave Event

Sea Level Rise (ft)	CBI-03	CBI-06	CBI-13	CBI-17	CBI-22	CBI-24
0.00	6.4	5.7	5.8	6.7	5.8	6.6
1.54 (2040)	7.9	8.0	7.8	8.3	8.5	7.1
3.54 (2070)	7.7	9.3	10.1	9.6	8.8	10.2

Table 5-17. Predicted Maximum Wave Run-up, in feet NAVD88, for the 100-Year Wave Event

Sea Level Rise (ft)	CBI-03	CBI-06	CBI-13	CBI-17	CBI-22	CBI-24
0.00	9.3	8.7	8.4	6.3	7.7	9.4
1.54 (2040)	9.3	10.4	8.1	9.2	8.6	10.7
3.54 (2070)	11.5	10.1	8.9	9.4	9.6	11.2

### 5.3.5 Individual Profiles

The next stage of analysis focused on the individual profiles and their predicted accretion and erosion as a result of the storm events and SLR scenarios.

Figure 5-3 illustrates the initial condition of one of the profiles, CBI-03, before the impact of a single storm event. A line for the mean sea level (MSL) elevation was added for reference. The SWL, at this start of each simulation, was derived from the NOAA water level data shown in Figure 5-1.

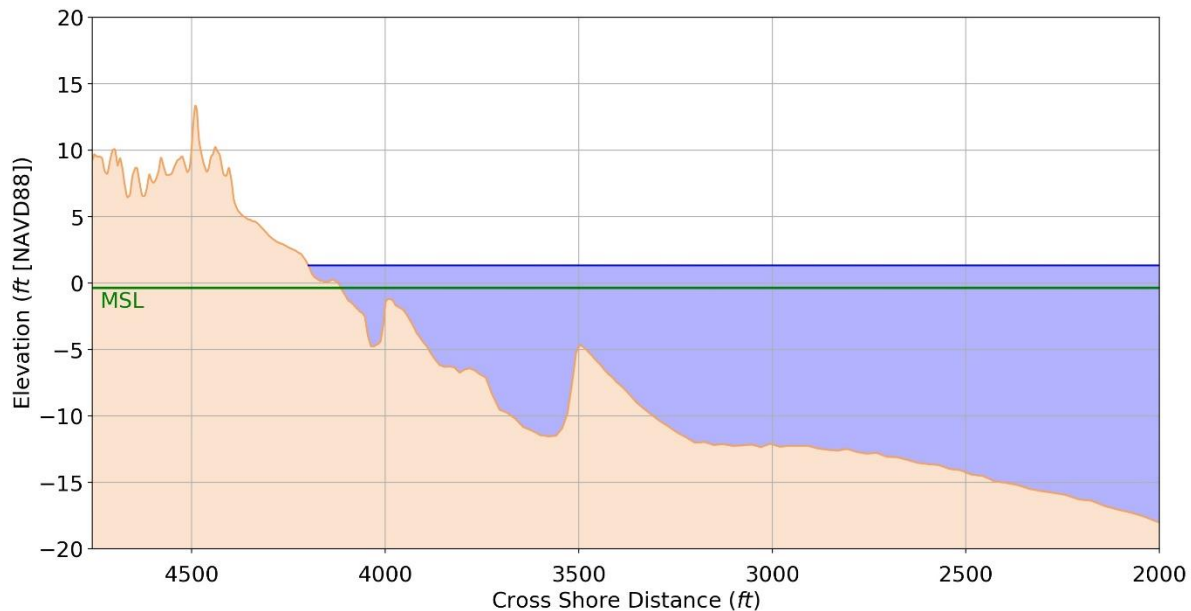


Figure 5-3. Initial Still Water Level and Bed Elevation for Profile CBI-03. MSL Datum Shown for Reference.

### 5.3.5.1 CBI-03

The predicted changes to the CBI-03 profile for the 2-, 10-, and 100-year wave events, across the three SLR scenarios, are shown in Figures 5-4 to 5-6. The beach width for CBI-03 decreased across the nine simulations. The change in beach width during the 100-year wave event under present SLR was largest for this storm scenario (Figure 5-6, top). Each of the storm events and SLR scenarios were predicted to decrease the beach width for this profile. The beach profile was steepened as a result of the breaking waves along the shoreline, thus reducing the distance from the dune toe to the shoreline. The smaller reductions in beach width during the SLR scenarios are a result of the waves breaking farther up the beach, and eroding sand, although sand is predicted to be deposited along the beach at or just below MSL. The 100-year wave event for the present and 2040 SLR scenarios had the largest change in beach width, and the smallest was during the 2-year and 10-year wave events and the 2070 SLR scenario.

The primary factor in the predicted decreases in beach width across the 9 simulations was the retreat of the shoreline position. The dune toe was only impacted during the 100-year wave event for the 2070 SLR scenario, when the waves and the water levels were the highest. As a note, the foredune was predicted to erode during the 100-year wave event and the 2070 SLR scenario, though this was not shown in the dune crest height tables presented above since it's not the highest dune along the profile (Figure 5-6, bottom).

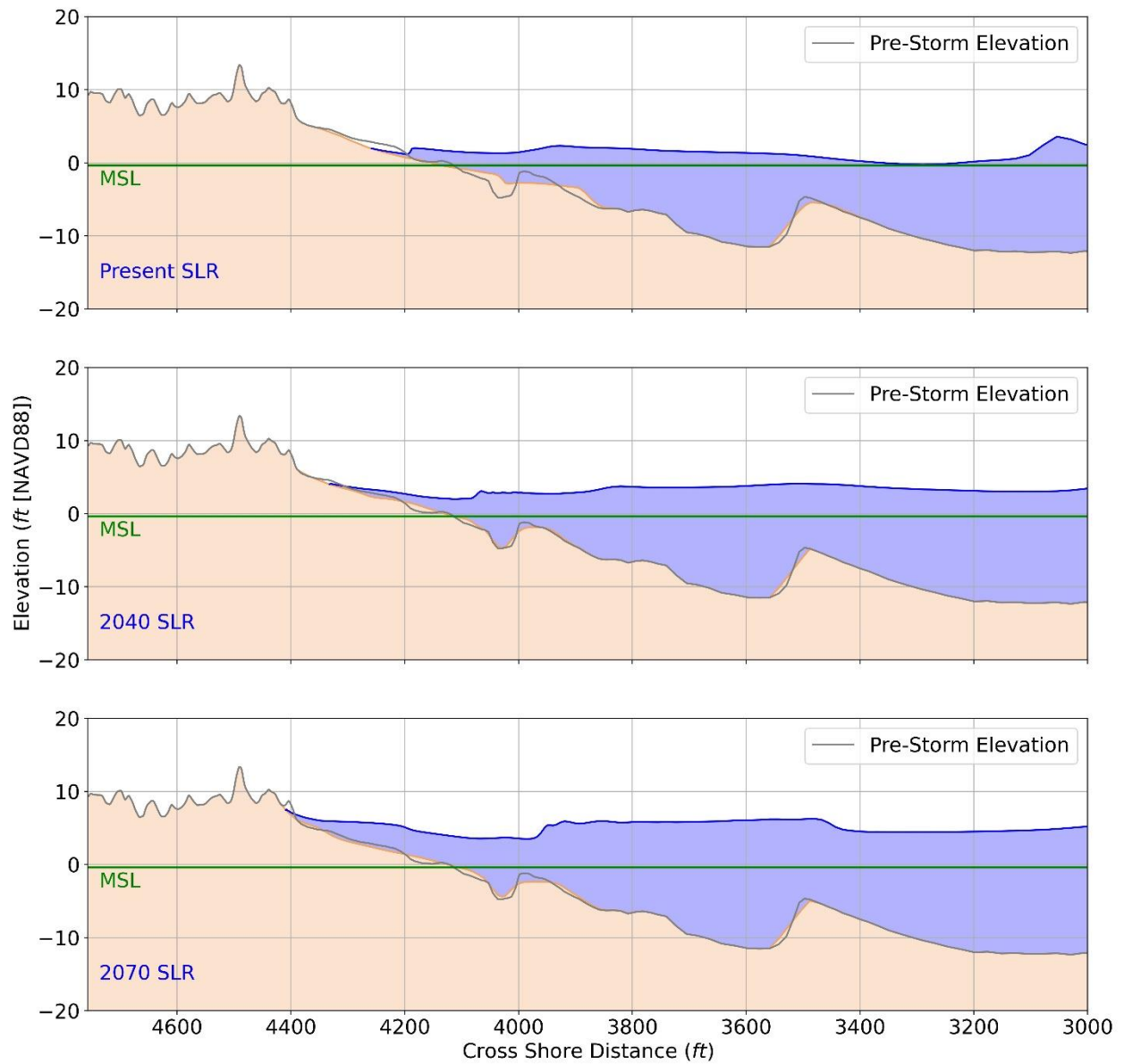


Figure 5-4. Predicted Shoreline Elevation for CBI-03 after 30 Hours of Exposure to a 2-Year Storm Event and 3 SLR Scenarios

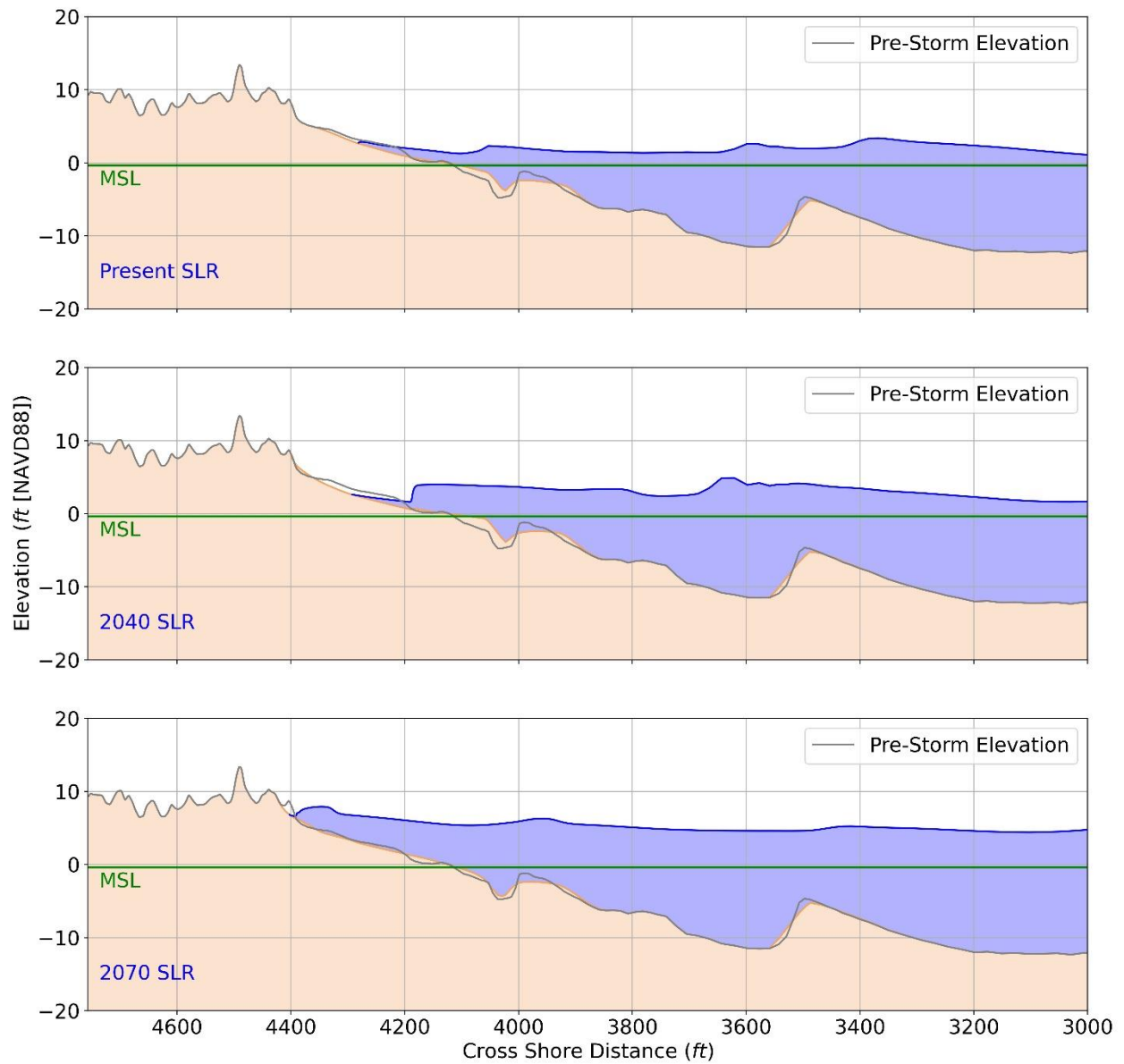


Figure 5-5. Predicted Shoreline Elevation for CBI-03 after 30 Hours of Exposure to a 10-Year Storm Event and 3 SLR Scenarios

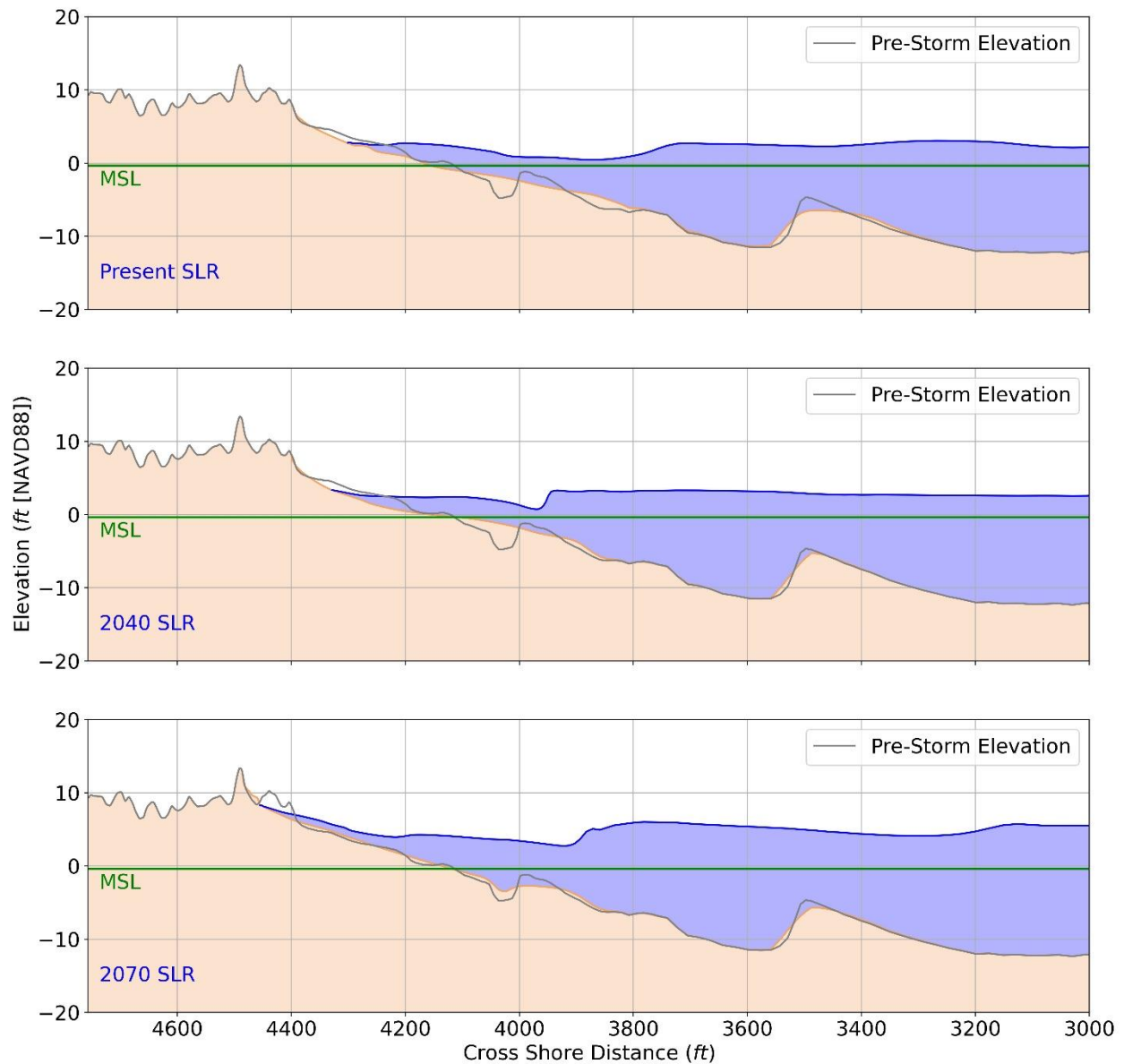


Figure 5-6. Predicted Shoreline Elevation for CBI-03 after 30 Hours of Exposure to a 100-Year Storm Event and 3 SLR Scenarios

### 5.3.5.2 CBI-06

The predicted changes to the CBI-06 profile for the 2-, 10-, and 100-year wave events, across the three SLR scenarios, are shown in Figures 5-7 to 5-9. The beach width was predicted to increase for the nine simulations along CBI-06, although as discussed earlier, the largest increase in beach width during the 10-year wave event was due to a large amount of erosion on the foredune (Figure 5-8, bottom). A similar beach width increase was predicted for the 100-year wave event and 2070 SLR scenario, a result of the retreating dune toe (Figure 5-9, bottom).

The primary factor in the predicted increases in beach width across the nine simulations was the advancement in the shoreline position. The dune toe was only impacted during the 10- and 100-year wave events for the 2070 SLR scenario, when the waves and the water levels were the highest. Interestingly, the foredune was predicted to erode during the 10-year wave event and the 2070 SLR scenario, though this was not shown in the dune crest height tables presented above since it's not the highest dune along the profile (Figure 5-8, bottom). The reason for the 10-year wave event causing foredune erosion and not during the 100-year wave event, with the same SLR scenario, is a result of the influence of bathymetry and topography on the breaking waves. Smaller waves, representative of those during the 10-year wave event, can travel closer to shore before breaking especially with higher sea levels. These waves would likely break closer to the foredune, causing the predicted erosion. Overtopping of the foredune was predicted for the 100-year wave event and the 2070 SLR scenario, though the foredune was not eroded. This is likely the reason for the dune toe change table showing a similar impact as the 10-year wave event (Table 5-11).

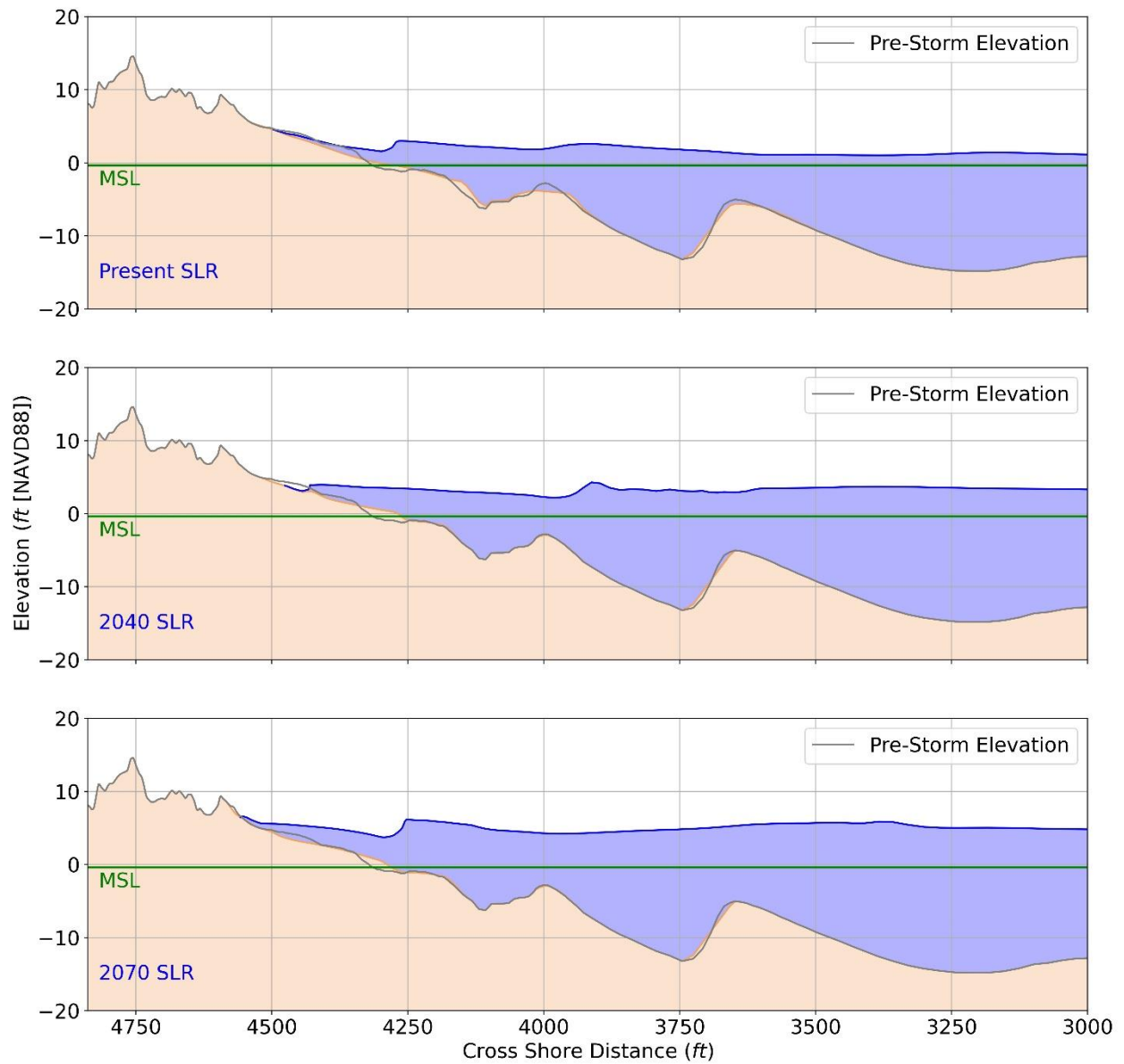


Figure 5-7. Predicted Shoreline Elevation for CBI-06 after 30 Hours of Exposure to a 2-Year Storm Event and 3 SLR Scenarios

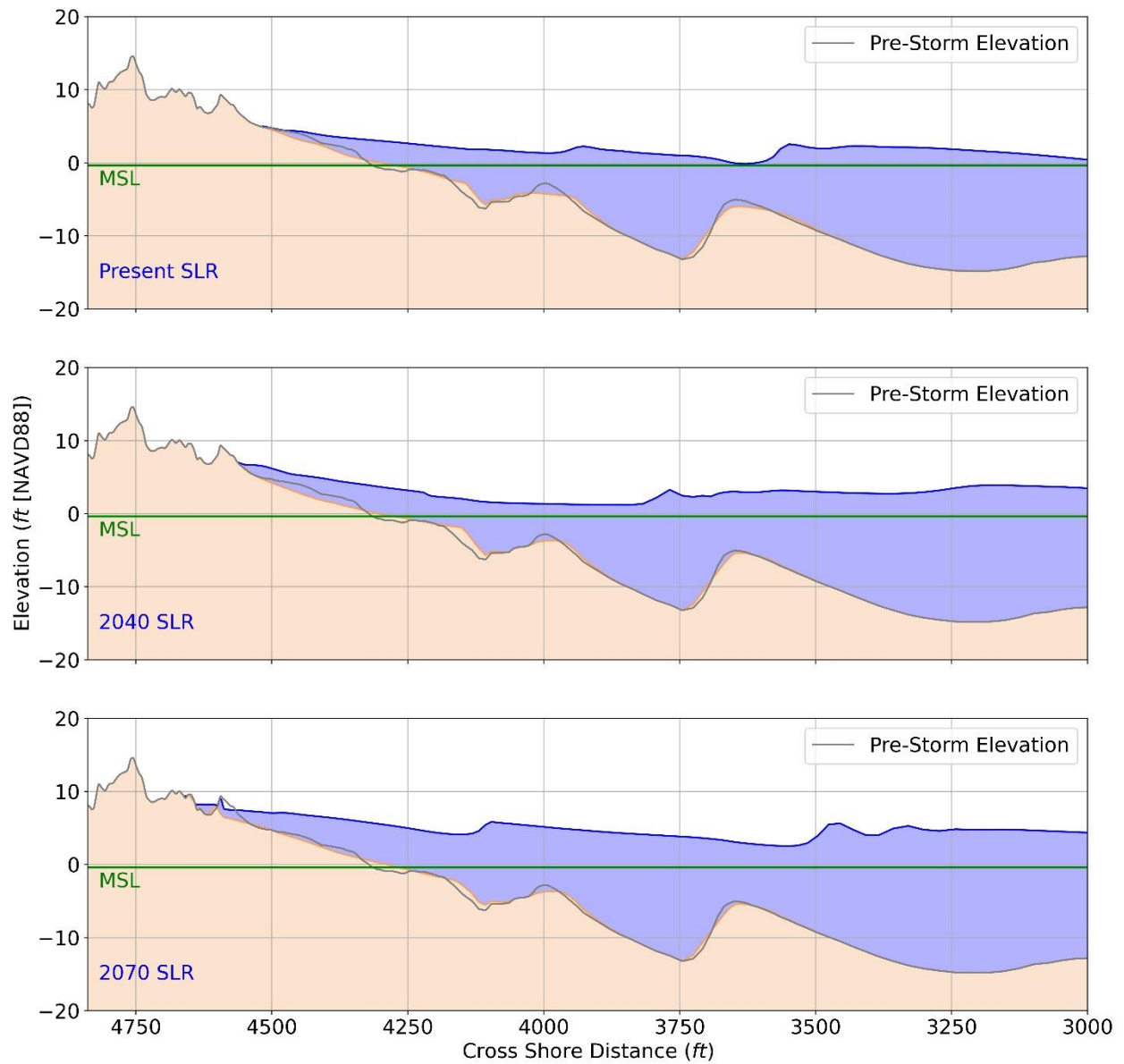


Figure 5-8. Predicted Shoreline Elevation for CBI-06 after 30 Hours of Exposure to a 10-Year Storm Event and 3 SLR Scenarios

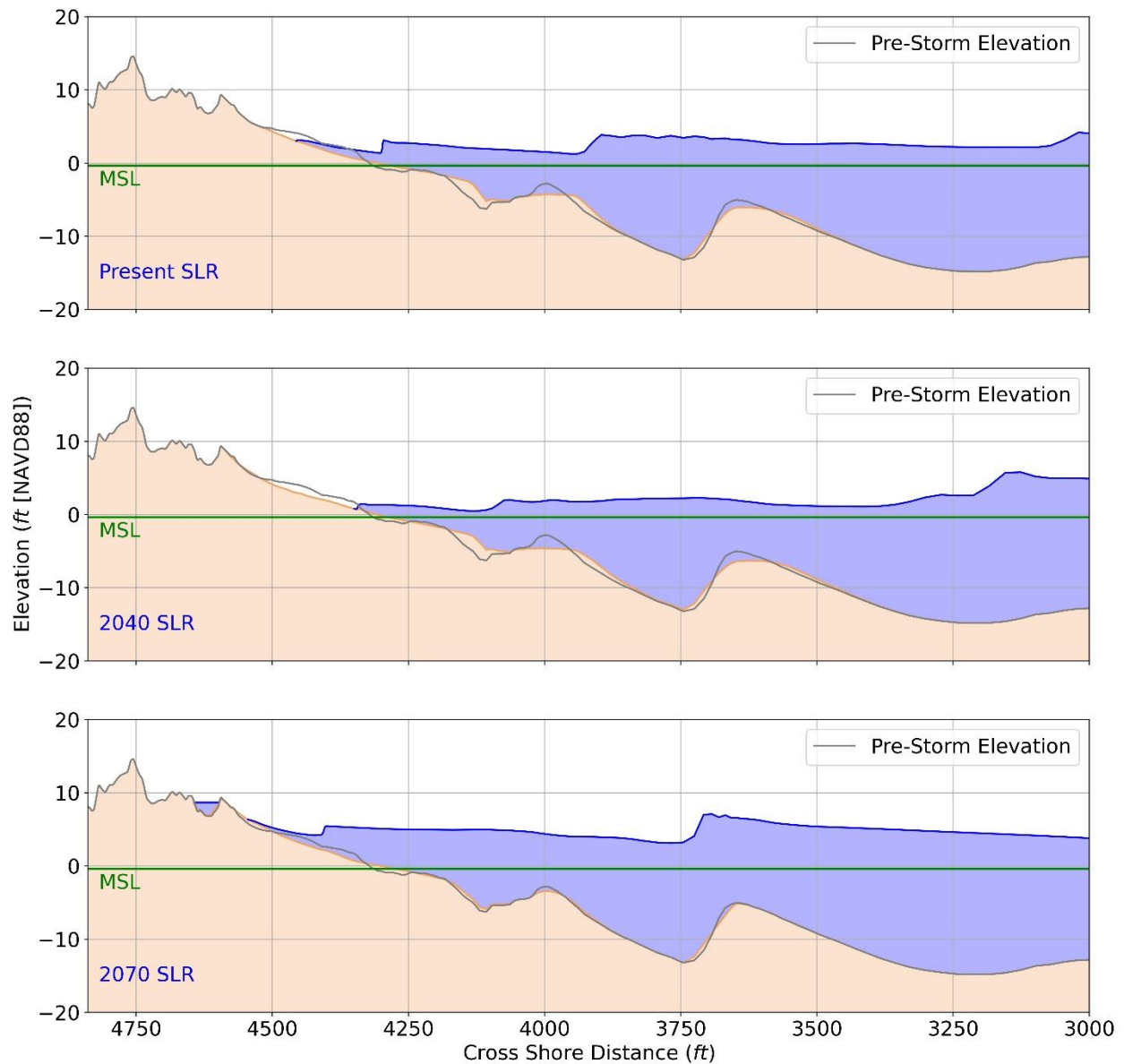


Figure 5-9. Predicted Shoreline Elevation for CBI-06 after 30 Hours of Exposure to a 100-Year Storm Event and 3 SLR Scenarios

### 5.3.5.3 CBI-13

The predicted changes to the CBI-13 profile for the 2-, 10-, and 100-year wave events, across the SLR scenarios, are shown in Figures 5-10 to 5-12. Similar to CBI-06, the beach width for the nine simulations along CBI-13 is predicted to increase. The largest increase in beach width occurred during the 100-year wave event and the 2070 SLR scenario, although this was again as a result of a retreat of the dune toe (Figure 5-12, bottom). Most of the other simulations had a similar retreat of the dune toe, resulting in the predicted increase in beach width.

The shoreline position and dune toe position were shown to generally advance and retreat, respectively, for CBI-13. This was likely a result of erosion of the foredune and material subsequently being deposited on the beach, resulting in the increases in beach width. The foredune was predicted to have some erosion during the 2- and 10-year wave events and the 2070 SLR scenario, though this was not shown in the dune crest height tables presented above since it's not the highest dune along the profile (Figures 5-10 and 5-11, bottom). Overtopping of the foredune was predicted during the 100-year wave event and the 2040 and 2070 SLR scenarios (Figure 5-12, middle and bottom).

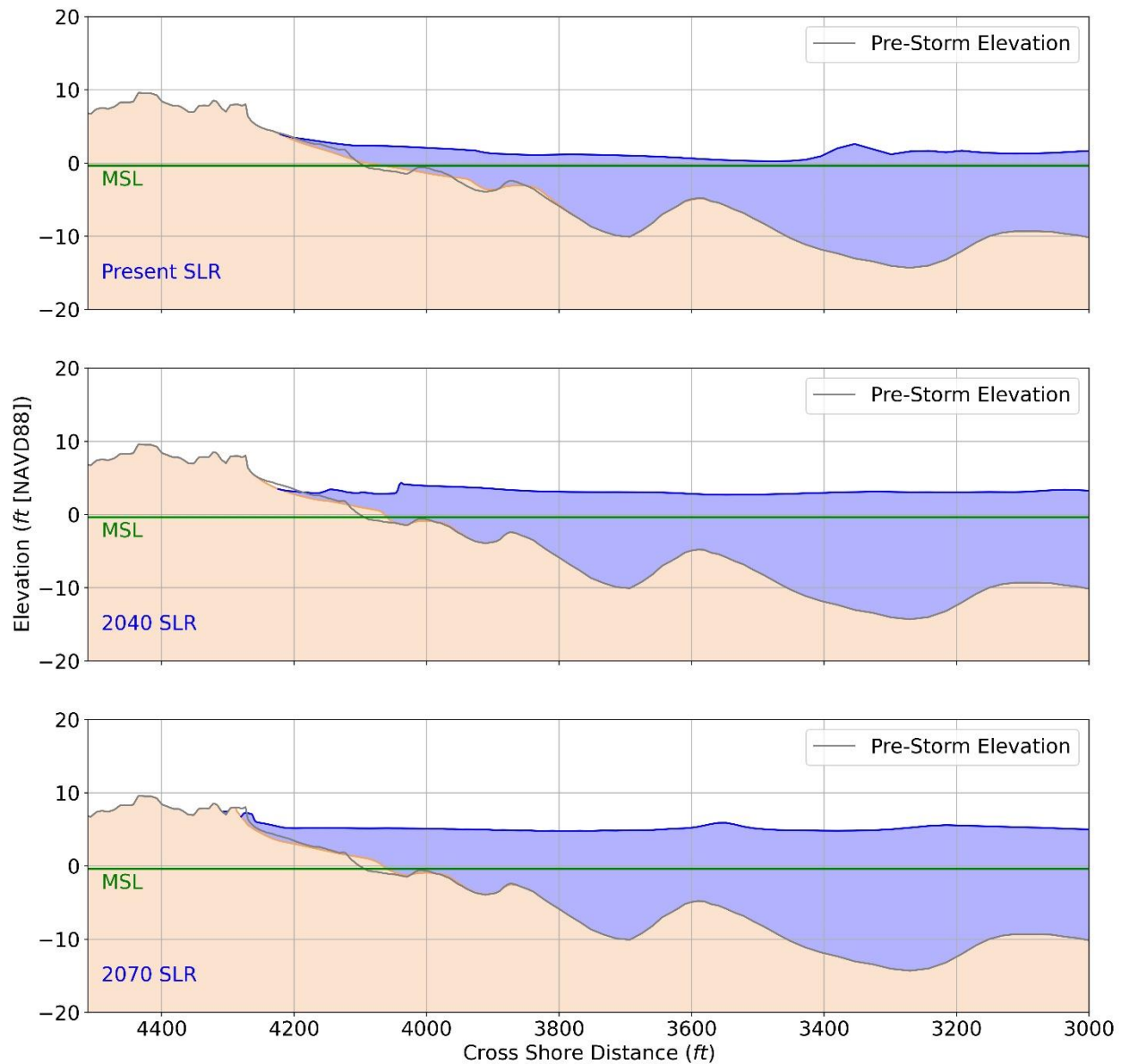


Figure 5-10. Predicted Shoreline Elevation for CBI-13 after 30 Hours of Exposure to a 2-Year Storm Event and 3 SLR Scenarios

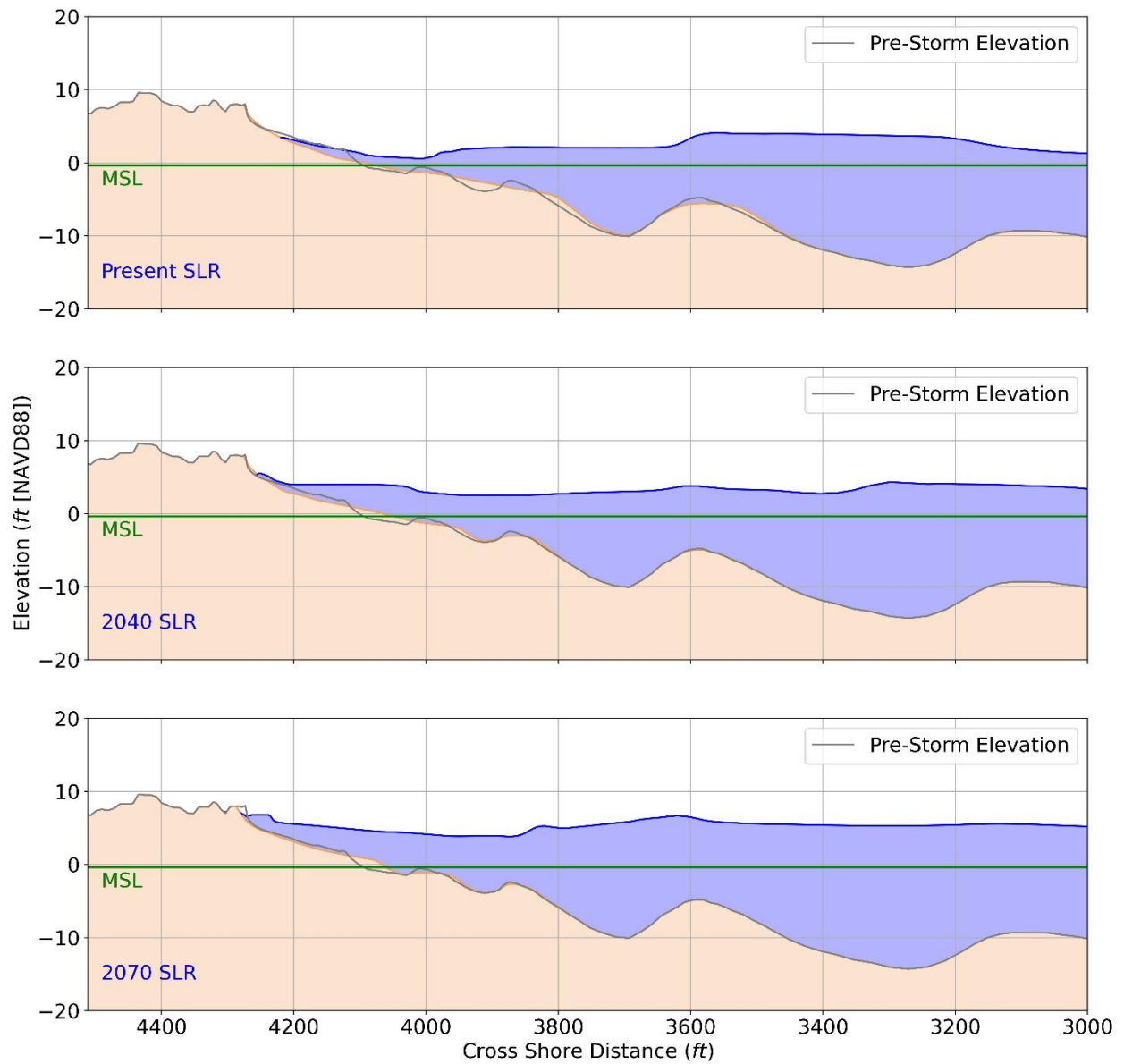


Figure 5-11. Predicted Shoreline Elevation for CBI-13 after 30 Hours of Exposure to a 10-Year Storm Event and 3 SLR Scenarios

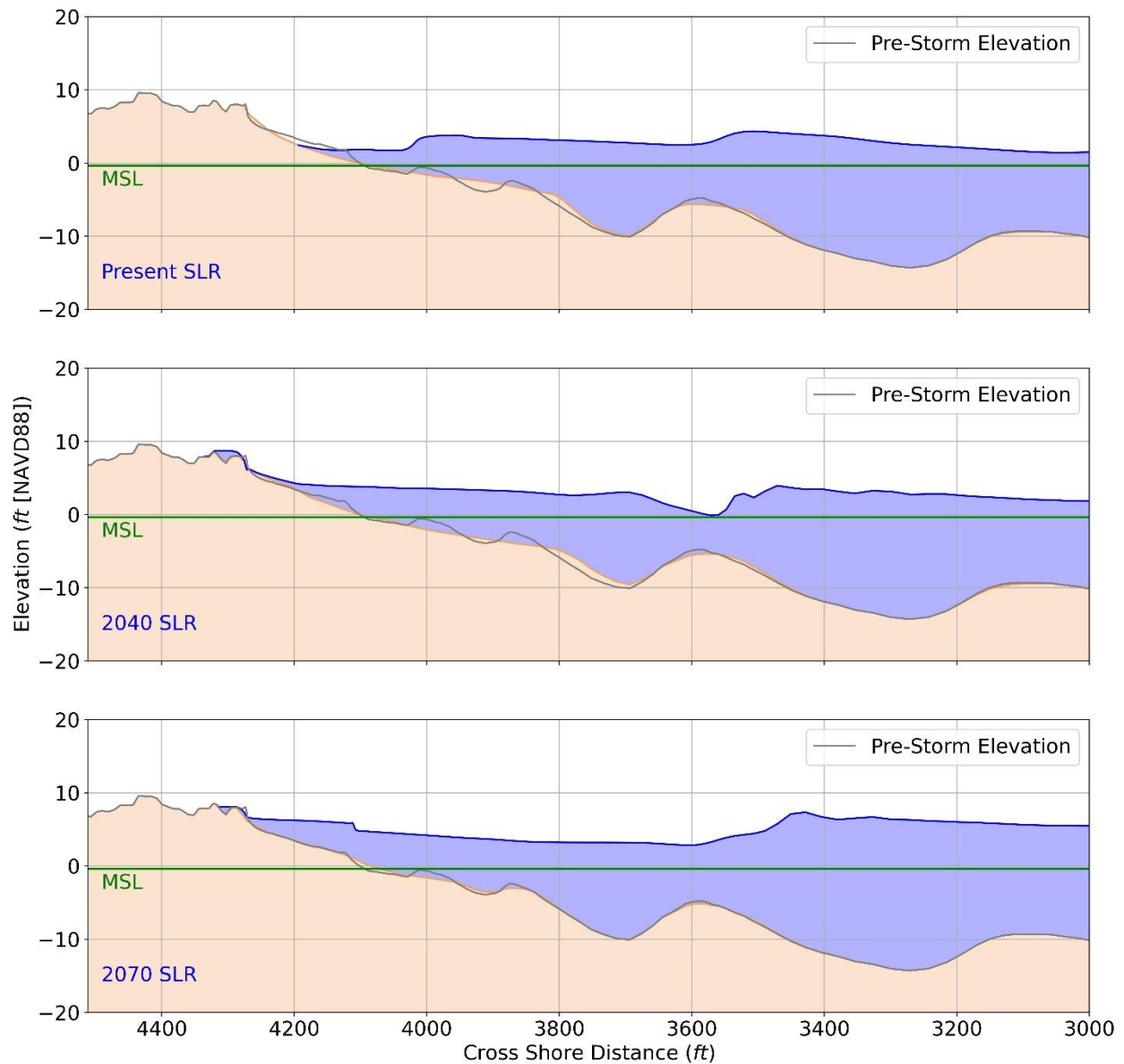


Figure 5-12. Predicted Shoreline Elevation for CBI-13 after 30 Hours of Exposure to a 100-Year Storm Event and 3 SLR Scenarios

#### 5.3.5.4 CBI-17

The predicted changes to the CBI-17 profile for the 2-, 10-, and 100-year wave events, across the SLR scenarios, are shown in Figures 5-13 to 5-15, respectively. A decreasing beach width was predicted for all but three of the CBI-17 simulations. One of those three simulation had no predicted change in beach width, and the remaining two had changes up to 6.6 ft. The largest changes in beach width occurred during the 100-year wave event under the present and 2040 SLR scenarios. This is a result of a steepening of the lower beach, and material deposited

seaward of the shoreline, below MSL (Figure 5-14 and Figure 5-15, top). The shoreline position was the primary factor in the decrease in beach width along this profile. Four of the nine simulations along this profile had predicted changes to the dune toe position. Three of those four occurred during the 2070 SLR scenario, and the largest occurred during the 100-year wave event and the 2040 SLR scenario. No beach width change was predicted for the 2-year wave event and 2070 SLR scenario (Figure 5-13, bottom), though the profile along the lower beach was altered.

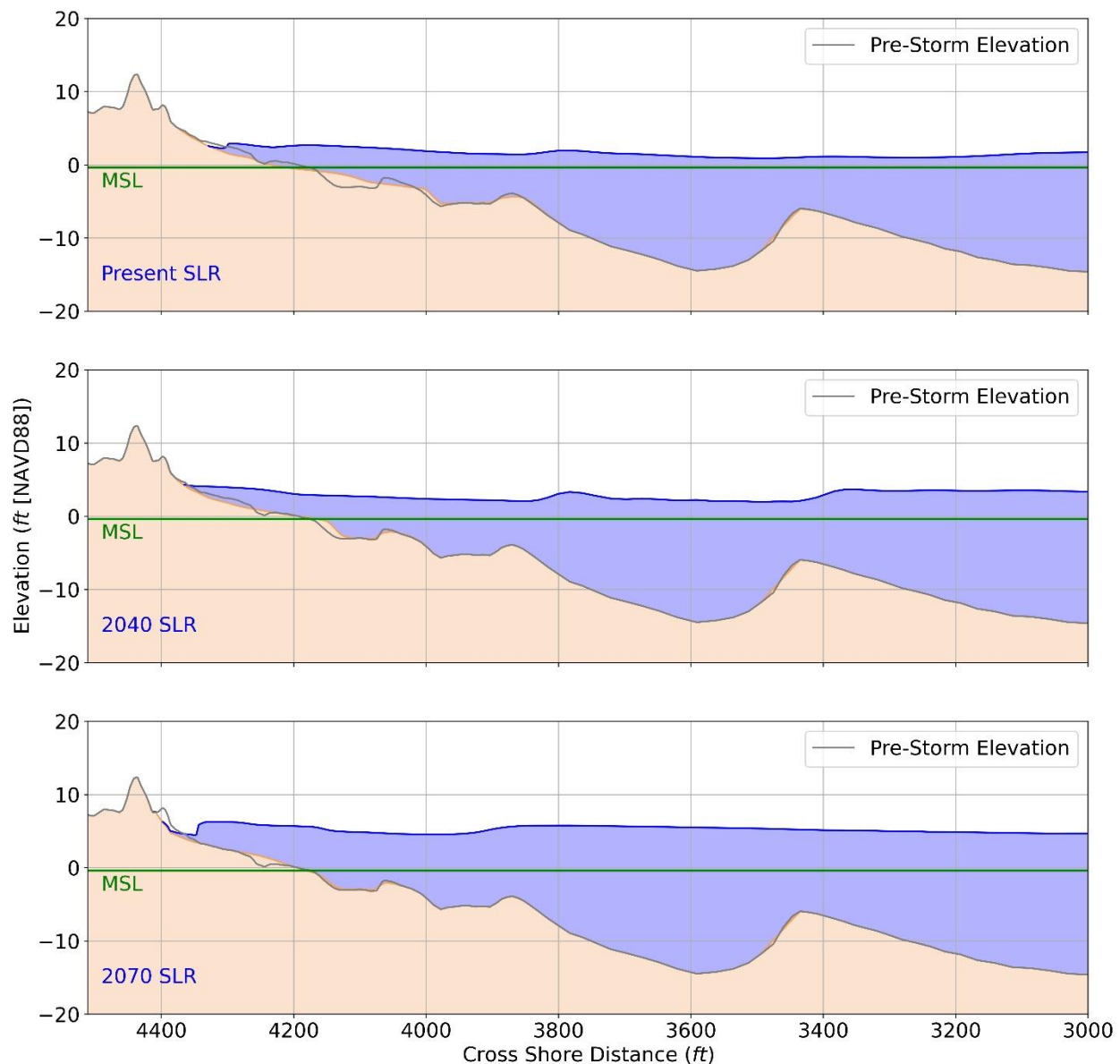


Figure 5-13. Predicted Shoreline Elevation for CBI-17 after 30 Hours of Exposure to a 2-Year Storm Event and 3 SLR Scenarios

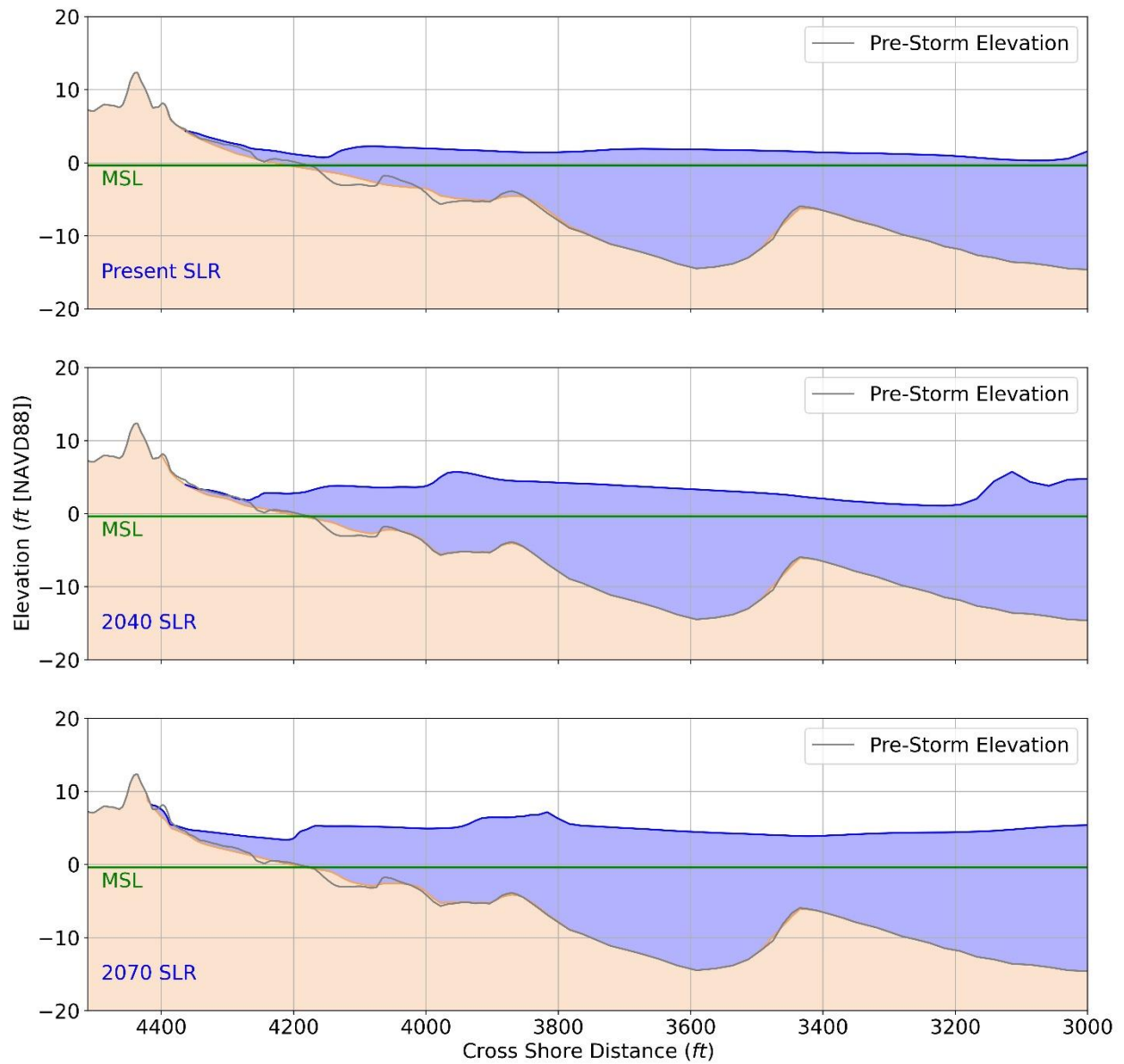


Figure 5-14. Predicted Shoreline Elevation for CBI-17 after 30 Hours of Exposure to a 10-Year Storm Event and 3 SLR Scenarios

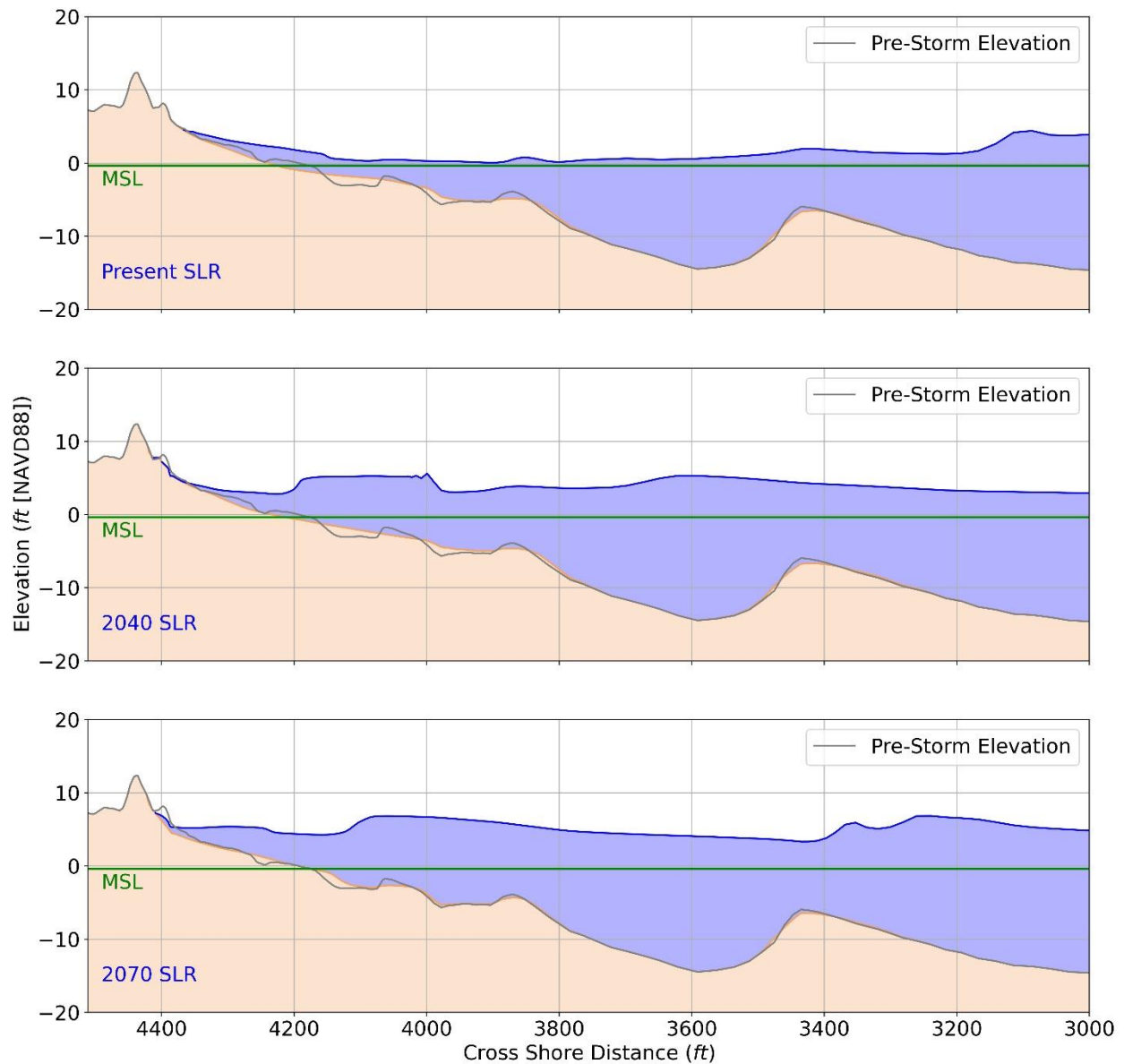


Figure 5-15. Predicted Shoreline Elevation for CBI-17 after 30 Hours of Exposure to a 100-Year Storm Event and 3 SLR Scenarios

### 5.3.5.5 CBI-22

The predicted changes to the CBI-22 profile for the 2-, 10-, and 100-year wave events, across the SLR scenarios, are shown in Figures 5-16 to 5-18. An increasing beach width was predicted for each of the CBI-22 simulations, except one. The increasing beach width was generally a result of an advancing shoreline position and retreat of the dune toe.

Interestingly, the 10-year storm event under present SLR conditions predicted a larger amount of erosion along the foredune as compared to the 100-year storm event (Figure 5-17). This is a result of the influence of bathymetry and topography on the wave energy. Smaller waves can travel closer to shore before breaking, especially with varying water levels. At the offshore point of the profile, the 100-year wave height is higher than the 10-year wave height (Table 5-2). As a result, the larger offshore wave of the 100-year event comes in contact with the seafloor at a deeper depth and will break, expelling its energy before rushing up to the foredune, thus reducing the potential for erosion. The 10-year offshore wave will break closer to the shoreline, thus increasing the potential for erosion. The importance of this finding is that more frequent wave events, rather than larger waves, could cause increased potential for coastal erosion. However, the occurrence of this is dependent on the local bathymetry as most of the other selected profiles were predicted to have larger amounts of erosion during the 100-year storm event, as would be expected.

The entire dune system was predicted to erode in four of the nine simulations at CBI-22, also confirmed in the dune crest height tables (Tables 5-12 to 5-14). The erosion was only predicted for the 2070 SLR scenario for the 2- and 10-year wave events (Figures 5-16 and 5-17, bottom). For the 100-year wave event, the dune erosion was predicted for the 2040 and 2070 SLR scenarios (Figure 5-18, middle and bottom). While the magnitude of the change in dune crest elevations were similar for these four simulations, upon closer inspection of the figures below, the new eroded profile is different, except for the height of the dune crest.

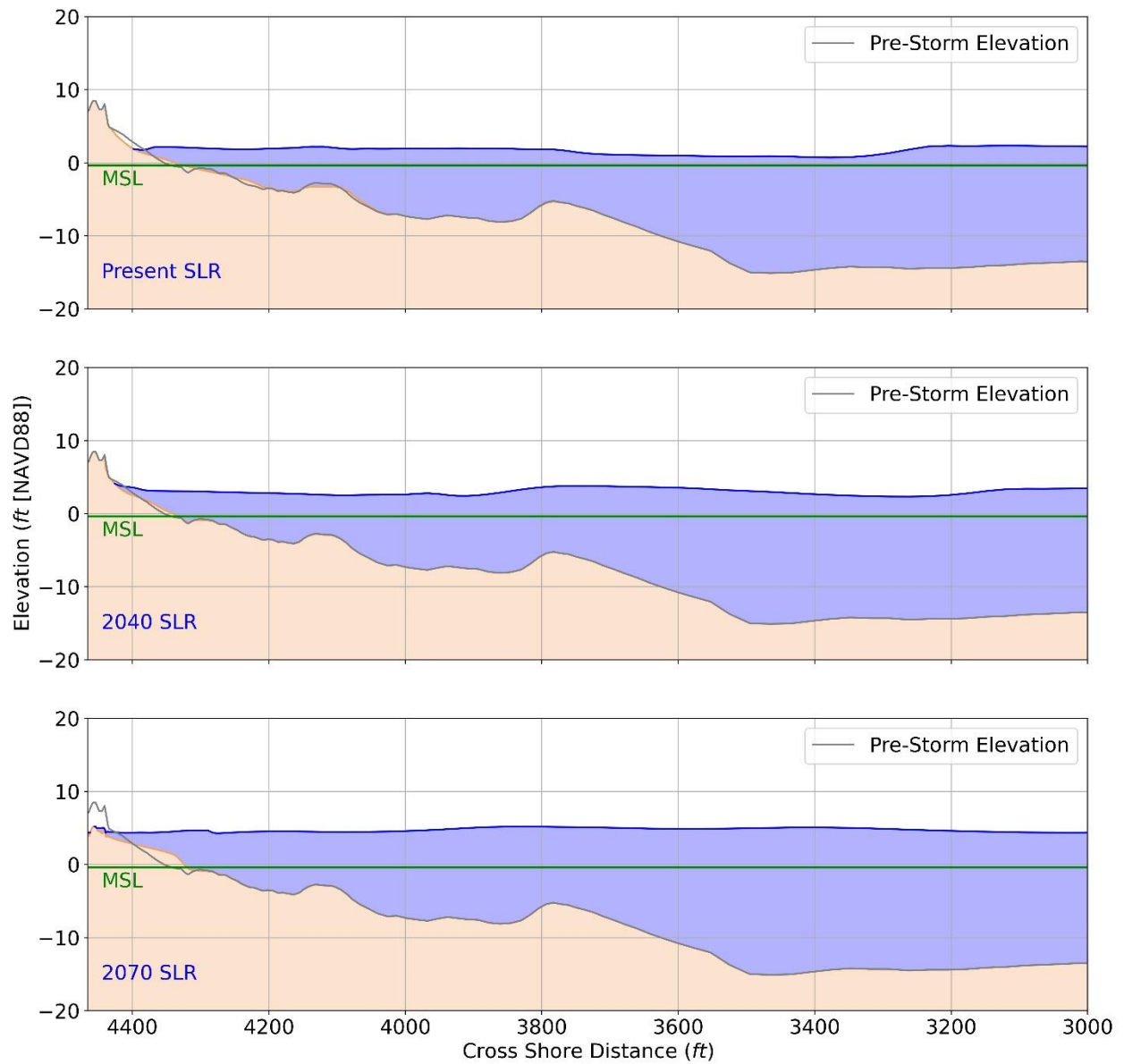


Figure 5-16. Predicted Shoreline Elevation for CBI-22 after 30 Hours of Exposure to a 2-Year Storm Event and 3 SLR Scenarios

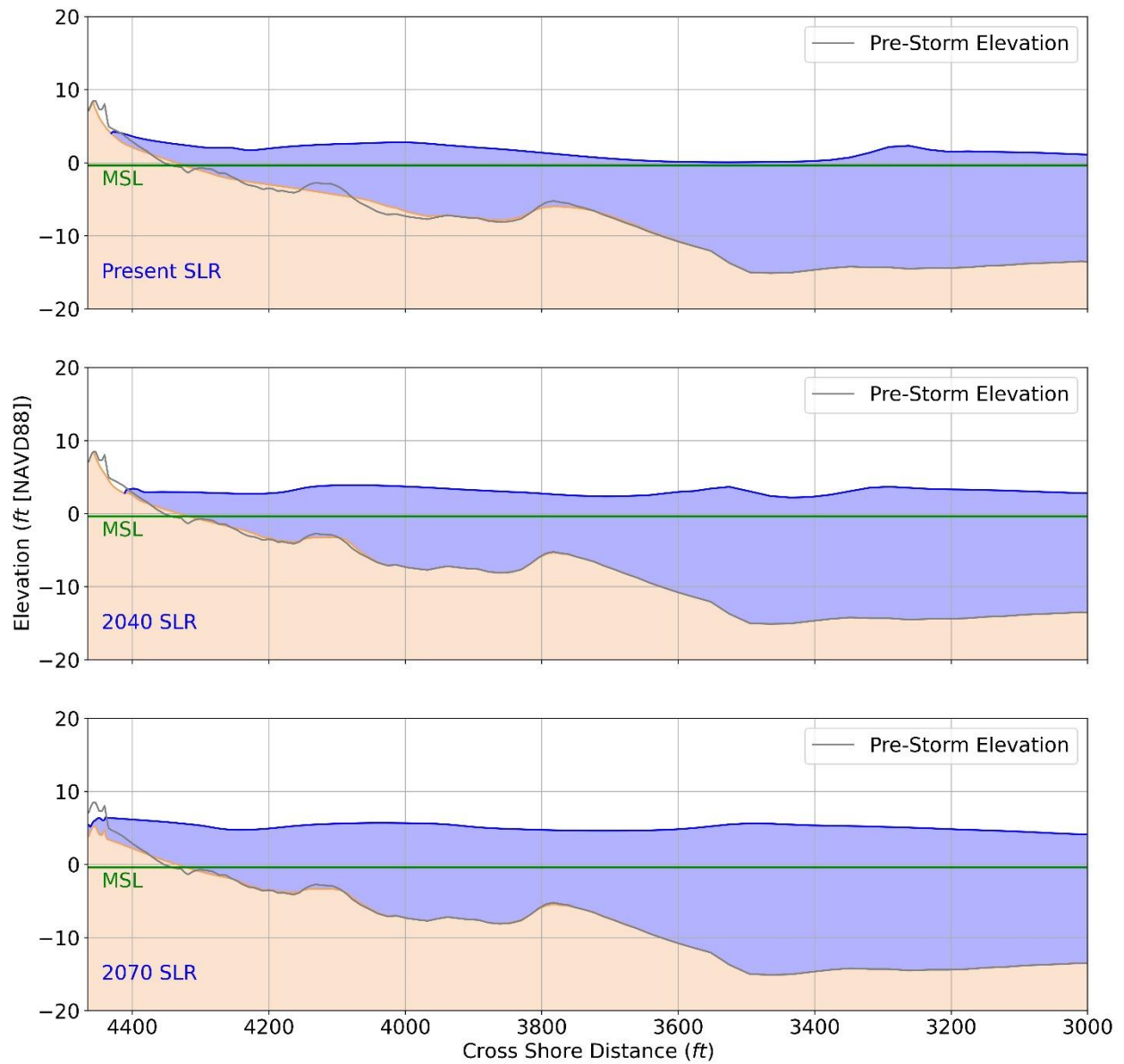


Figure 5-17. Predicted Shoreline Elevation for CBI-22 after 30 Hours of Exposure to a 10-Year Storm Event and 3 SLR Scenarios

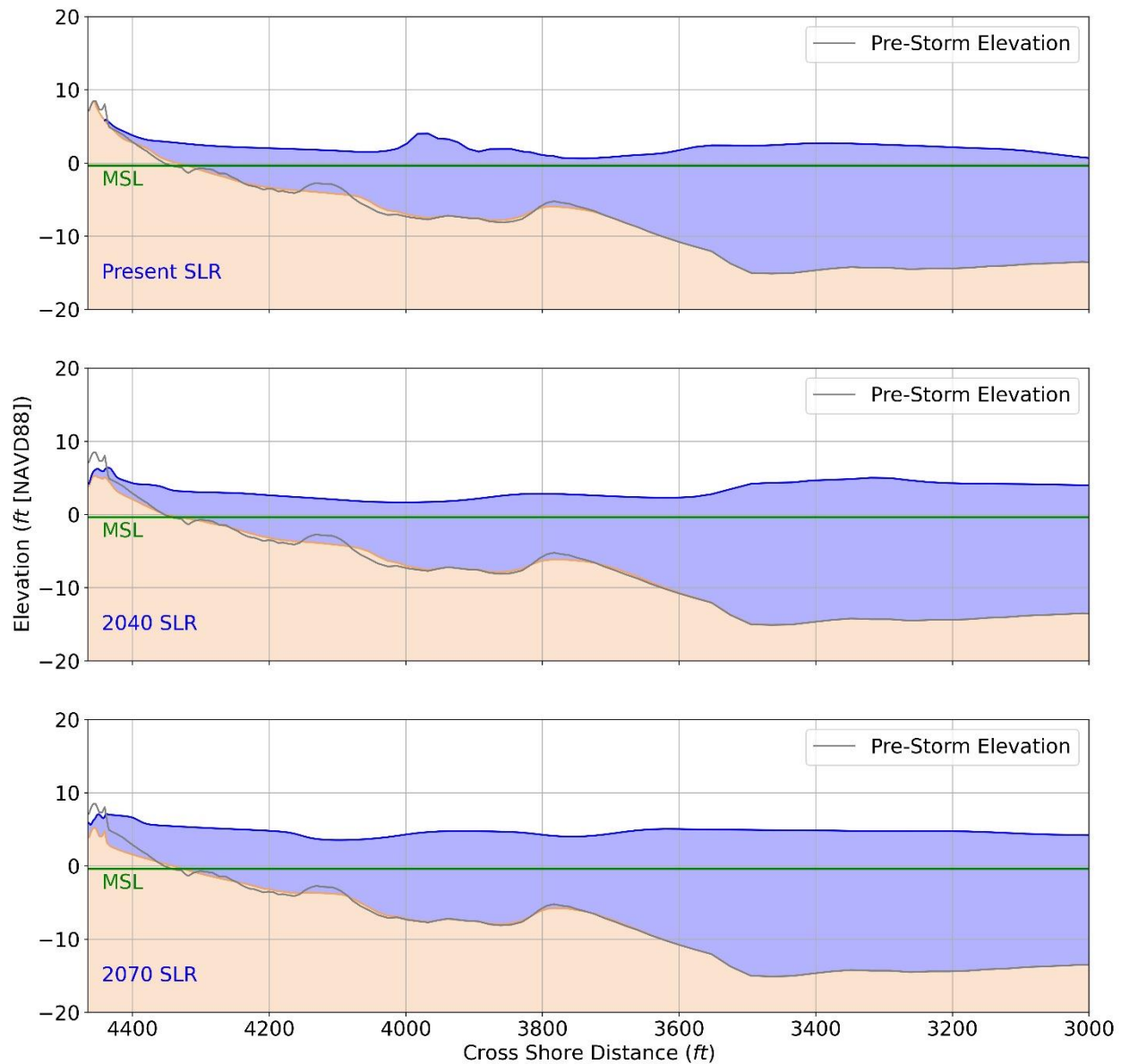


Figure 5-18. Predicted Shoreline Elevation for CBI-22 after 30 Hours of Exposure to a 100-Year Storm Event and 3 SLR Scenarios

### 5.3.5.6 CBI-24

The predicted changes to the CBI-24 profile for the 2-, 10-, and 100-year wave events, across the SLR scenarios, are shown in Figures 5-19 to 5-21, respectively. This profile was predicted to have the largest decreases in beach width, and is the northernmost profile that was evaluated with XBeach. During the 2-year wave event, the beach width was predicted to increase for the present and 2070 SLR scenarios, a result of a shoreline position advancement and, in the case of the 2070 SLR scenario, retreating dune toe. For the 10- and 100-year wave events, the beach

width was predicted to decrease, primarily as a result of retreat of the shoreline position. This is a result of a steepening of the shoreface due to erosion and deposition of material seaward of the shoreline, below MSL.

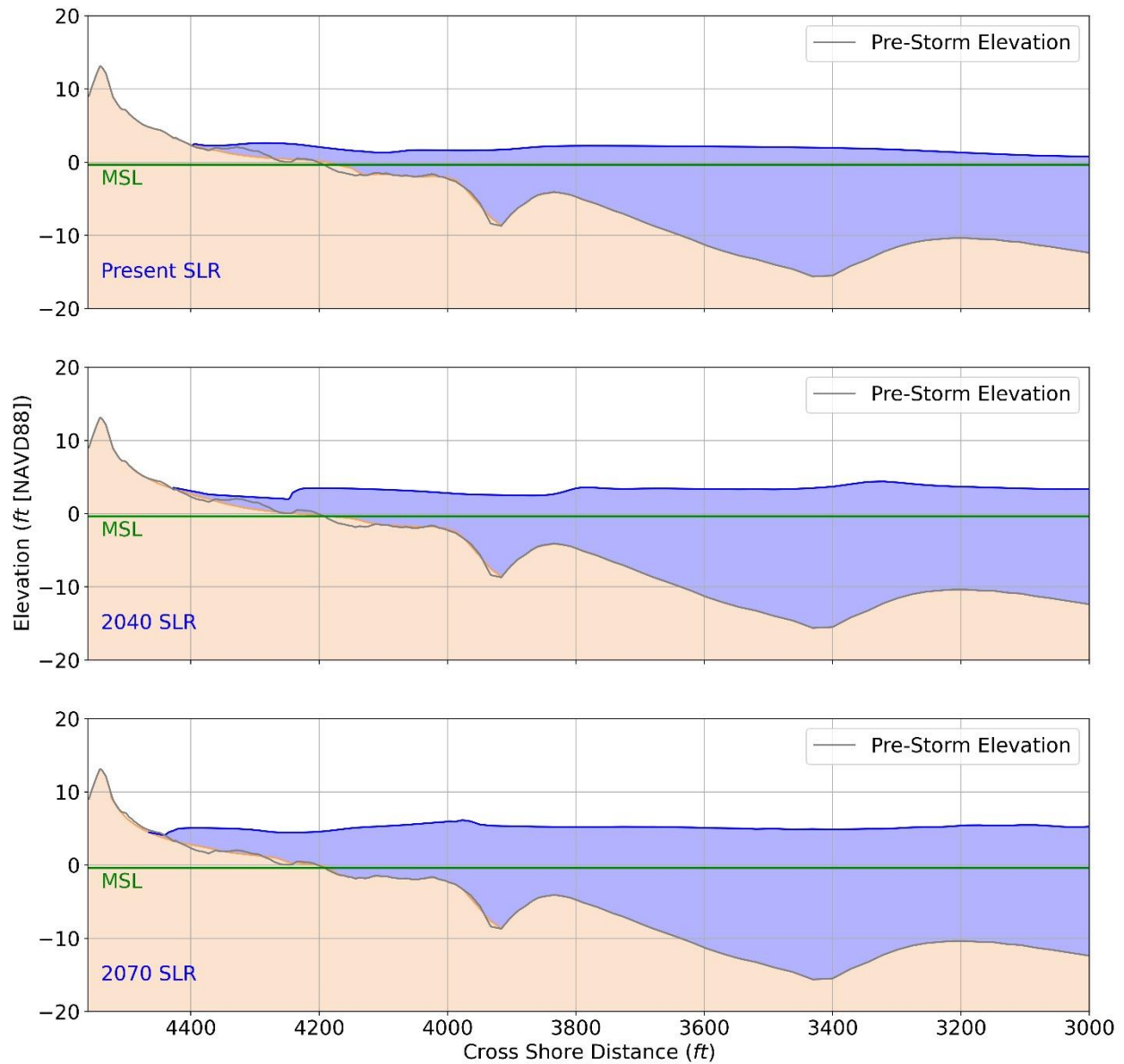


Figure 5-19. Predicted Shoreline Elevation for CBI-24 after 30 Hours of Exposure to a 2-Year Storm Event and 3 SLR Scenarios

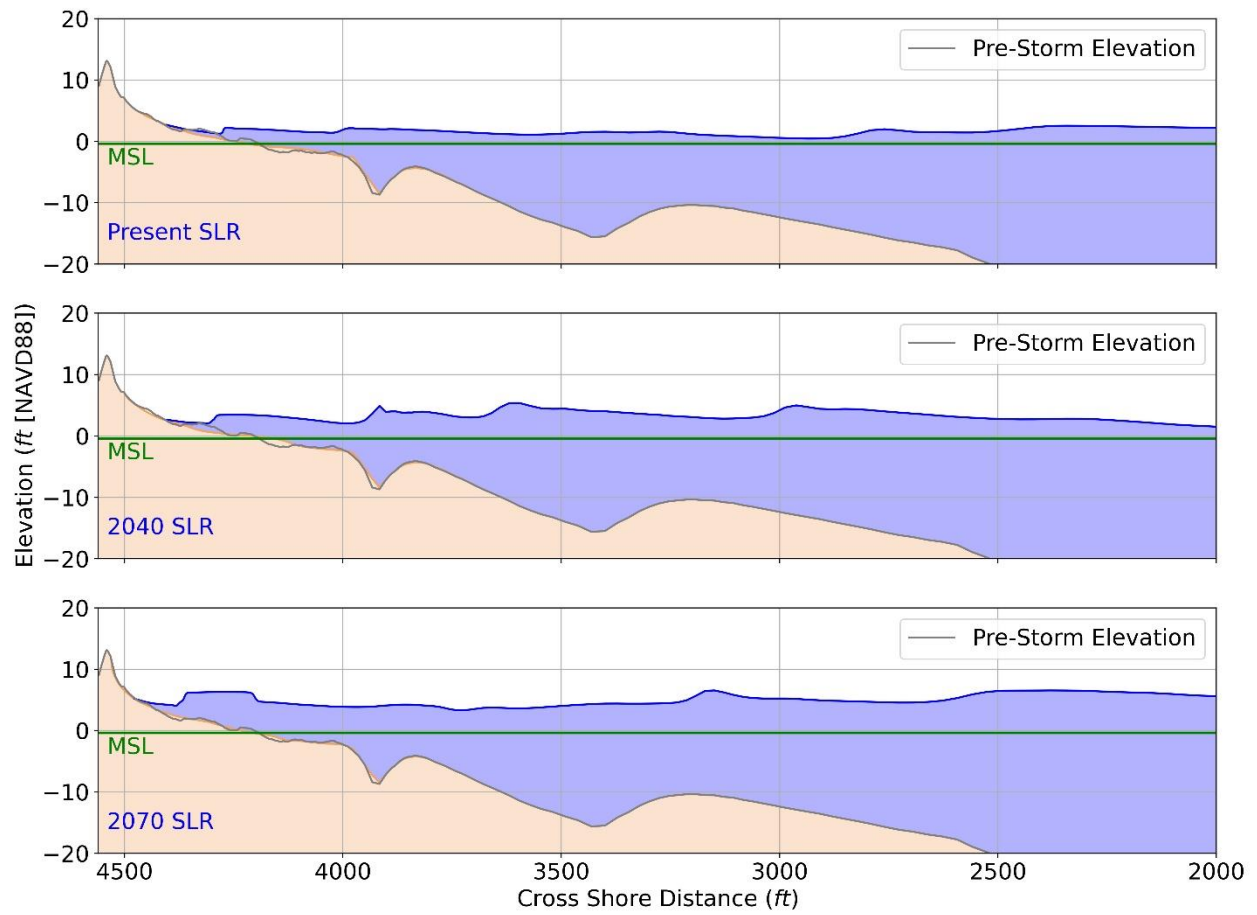


Figure 5-20. Predicted Shoreline Elevation for CBI-24 after 30 Hours of Exposure to a 10-Year Storm Event and 3 SLR Scenarios

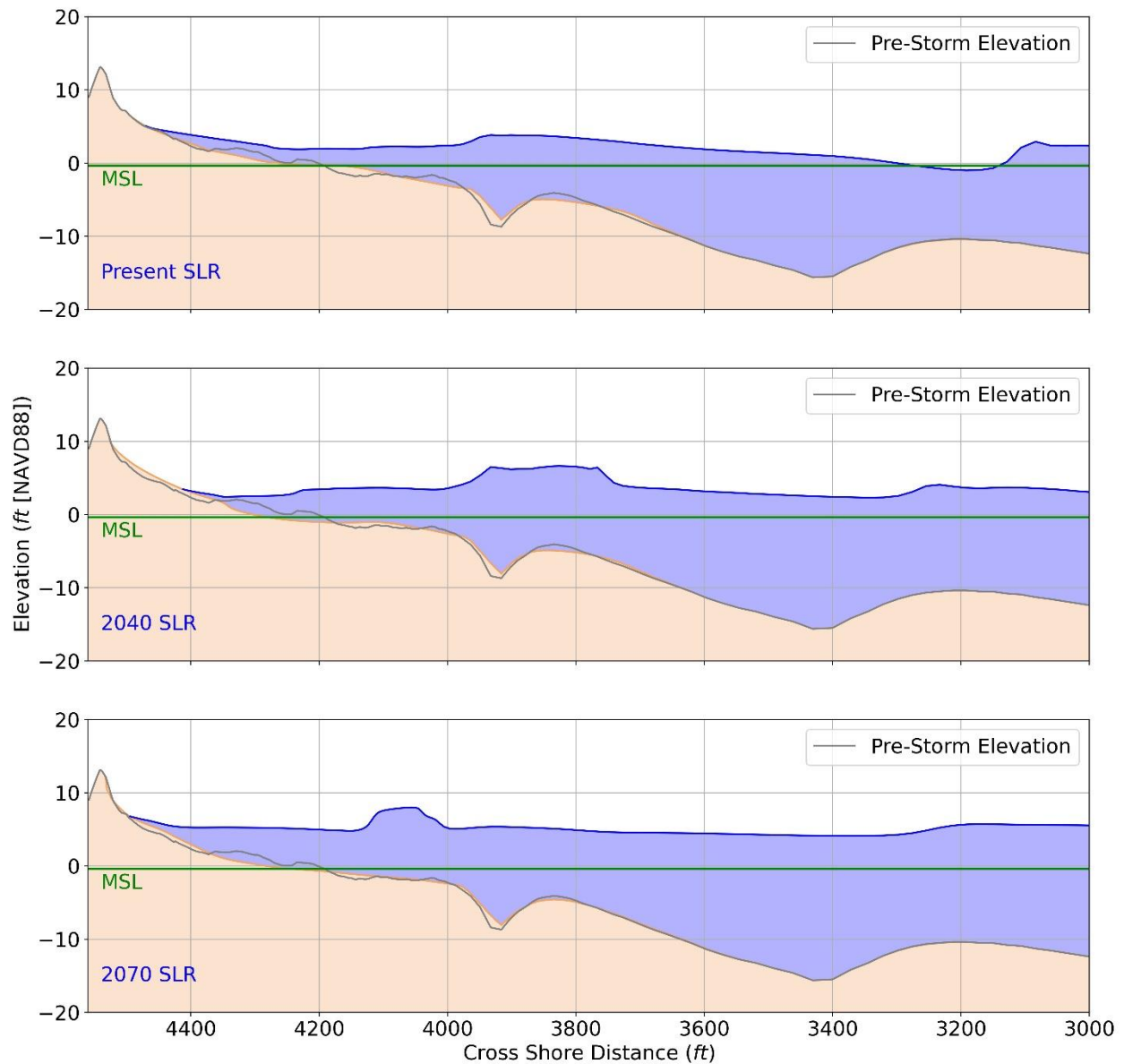


Figure 5-21. Predicted Shoreline Elevation for CBI-24 after 30 Hours of Exposure to a 100-Year Storm Event and 3 SLR Scenarios

## 5.4 MODEL UNCERTAINTY

Model grid resolution and bathymetry interpolation lead to potential sources of model uncertainty. Modeled bathymetry within a grid cell, while reflective of the mean bathymetry measured using an echo sounder, might be shallower or deeper in certain regions of the cell, leading to enhanced sub-grid-scale erosion/deposition in nature that is not captured by the model.

In addition, uncertainties can arise when assigning values to the sediment bed properties. Sediment bed properties were defined uniformly and contain primarily sand. Variability of these properties within a profile can lead to variability in predicted erosion and accretion, and hence uncertainty in model predictions. The effect of this variability can be evaluated by undertaking sensitivity tests that vary the sediment bed composition during the selected storm events.

However, the net effect of these uncertainties on the short-term sediment transport along each of the profiles is assumed minimal relative to the predictions of erosion and accretion, and conform to the scope of this project. Additionally, uniform sediment bed definition along the length of each profile is assumed based on limited data and may not be explicitly representative of erosion parameters in a specific area. Since the modeling represents acute storm events, the accuracy of predicted changes in bottom elevation is only qualitatively evaluated against the survey data in terms of the model's ability to predict overall patterns of coastal erosion and accretion potential.

Finally, there are uncertainties associated with the auto-derivation of metrics from the model-output profiles. PyBeach uses a code written in Python, and although typical methods were used to extract the dune crest, dune toe, and shoreline, the results can be impacted by the complex topography of the dunes along the selected SPI profiles. However, this method was used to extract the same metrics from the actual survey data, and we qualitatively QA/QC'd outputs and results.

## 6 SUMMARY OF FINDINGS

In summary, there was a wide range of predicted changes for the selected profiles along SPI in response to the 2-, 10-, and 100-year wave events, and the present, 2040, and 2070 SLR scenarios. The overall findings of this study are bulleted below. As shown in the tables and figures previously presented, most of the predicted beach width change is due to changes in the shoreline position as opposed to changes in the dune toe position. In general, the predicted wave impacts for most of the 54 simulations are along the lower beachface, causing erosion or accretion at or near the shoreline, and the dune toe is not being eroded in most cases.

- CBI-06, CBI-13, and CBI-22 were predicted to have an increase in beach width, except in one of the simulations (the 10-year wave event with 2040 SLR for CBI-22).
  - Beach width increases are primarily a function of progradation of the shoreline from either erosion of the foredunes or deposition of sediment from either cross-shore or along-shore transport. Though, as stated in Section 5.1, in using XBeach in 1-D mode, the model domain represents a single shoreline profile, and longshore transport gradients are ignored.
- Predicted impacts to the foredune were more common in the more northerly profiles.
- The largest shoreline position retreat was predicted in CBI-24, the northernmost profile.
- As material was eroded from the foredune and lower beach, it was deposited offshore, just below MSL.
- Overtopping of the foredune occurred along multiple profiles, including CBI-03, CBI-06, CBI-13, and CBI-22, mostly during the 2070 SLR scenarios. However, only profile CBI-22 was predicted to have overtopping of the entire dune system.
- The largest changes (both erosion and accretion) do not necessarily occur during the largest storm events.

The predicted change in beach width, shoreline position, dune toe position, and the overall shape of the profile is representative of change during storm events. However, there are intervening years where portions of the system will move back to a dynamic equilibrium state after an acute event.

## **7 RECOMMENDATIONS AND NEXT STEPS**

The coastal hazard analysis of six selected profiles along South Padre Island, Texas, identifies key areas of future concern for the shoreline. In short, this study has identified predicted impacts of potential coastal change during storm events under future SLR along SPI. The next step is to integrate the findings of this study to inform coastal planning decisions.

The predicted maximum wave run-up values provide the indication to support maintaining a robust primary dune; run-up values during the 100-year storm events with moderate (2040) and high (2070) SLR are approaching elevations in which dune overtopping may occur. The practice of lowering dunes that exceed 10 ft in elevation will exacerbate overtopping, leading to more erosion of the dunes and potential inland flooding. It is widely accepted in the coastal literature that wide beaches, and wide and high dunes, optimally mitigate inland flooding and help to maintain a robust recreational resource. The modeling shows that when there is a wide beach and dune system, the impacts from storms plus SLR may erode the beach, but help prevent the dunes from severe impacts. Based on the modeled responses, as well as the past behavior of the system as described in the Phase 1 Report, it is recommended that a minimum dune elevation of 12.7 ft (higher than the largest predicted wave run-up elevation with a 10% safety factor) be maintained for the most resilient configuration at SPI. Ideal beach widths should be maintained with a minimum width of 200 ft, although greater width would provide more protection to the dunes. This resilient configuration will be evaluated against competing community interests (e.g., viewsheds) in the next phase.

The modeling results and historical analysis also support that having an intact continuous dune system is important to the resiliency of the system. In locations where dunes have been removed for recreation or other purposes, the system is inherently more vulnerable as large storm waves can reach the base of the buildings or infrastructure. Large storms may result in flooding of these community assets. The impact is not limited to the area where the dunes have been removed; up-rushing waves reaching a seawall or building may deflect off the hardened structure and push water laterally, causing erosion of the dunes along adjacent coastal reaches.

A similar, but smaller scale, vulnerability to storm waves and SLR is the numerous walkways through the dunes. During storms, especially with the elevated water levels associated with SLR, water flowing directly into the shore-perpendicular passages can result in lateral erosion of the adjacent dunes. Reducing the number of walkways, or having walkways converted to dune walkovers, would increase the resiliency of the system.

## 8 REFERENCES

- Appendini, C.M., A. Torres-Freyermuth, P. Salles, J. López-González, and E.T. Mendoza. 2014. Wave climate and trends for the Gulf of Mexico: A 30-yr wave hindcast. *Journal of Climate* 27(4):1619–1632.
- Point Blue and USGS. Our Coast Our Future (OCOFO). Web application, Petaluma, California. [www.ourcoastourfuture.org](http://www.ourcoastourfuture.org). Accessed November 1, 2021. Point Blue Conservation Science and U.S. Geological Survey.
- IPCC. 2021. Summary for Policymakers. In: *Climate Change 2021: The Physical Science Basis. Contribution of Working Group I to the Sixth Assessment Report of the Intergovernmental Panel on Climate Change*. V. Masson-Delmotte, P. Zhai, A. Pirani, S. L. Connors, C. Péan, S. Berger, N. Caud, Y. Chen, L. Goldfarb, M. I. Gomis, M. Huang, K. Leitzell, E. Lonnoy, J.B.R. Matthews, T. K. Maycock, T. Waterfield, O. Yelekçi, R. Yu, and B. Zhou (eds). Cambridge University Press. In Press.
- Nerem, R.S., B.D. Beckley, J.T. Fasullo, B.D. Hamlington, D. Masters, and G.T. Mitchum. 2018. Climate-change-driven accelerated sea-level rise detected in altimeter era. *Proceedings of the National Academy of Sciences* 115(9):2022–2025.
- Roelvink, D., A. Reniers, A.P. Van Dongeren, J.V.T. De Vries, R. McCall, and J. Lescinski. 2009. Modelling storm impacts on beaches, dunes and barrier islands. *Coastal Engineering* 56(11-12):1133–1152.
- Sweet, W.V., R.E. Kopp, C.P. Weaver, J. Obeysekera, R.M. Horton, E.R. Thieler, and C. Zervas. 2017. Global and regional sea level rise scenarios for the United States. NOAA Technical Report NOS CO-OPS 083. National Oceanic and Atmospheric Administration.